

Monitoring Supergiant Fast X-ray Transients with *Swift*. Results from the first year

P. Romano¹, L. Sidoli², G. Cusumano¹, V. La Parola¹, S. Vercellone¹, C. Pagani³,
L. Ducci^{4,2}, V. Mangano¹, J. Cummings⁵, H.A. Krimm^{5,6}, C. Guidorzi⁷, J.A. Kennea³,
E.A. Hoversten³, D.N. Burrows³, N. Gehrels⁵

¹INAF, Istituto di Astrofisica Spaziale e Fisica Cosmica, Via U. La Malfa 153, I-90146 Palermo, Italy

²INAF, Istituto di Astrofisica Spaziale e Fisica Cosmica, Via E. Bassini 15, I-20133 Milano, Italy

³Department of Astronomy and Astrophysics, Pennsylvania State University, University Park, PA 16802, USA

⁴Dipartimento di Fisica e Matematica, Università dell'Insubria, Via Valleggio 11, I-22100 Como, Italy

⁵NASA/Goddard Space Flight Center, Greenbelt, MD 20771, USA

⁶Universities Space Research Association, Columbia, MD, USA

⁷Dipartimento di Fisica, Università di Ferrara, Via Saragat 1, I-44100 Ferrara, Italy

Accepted 2009 July 07. Received 2009 July 07; in original form 2009 May 24

ABSTRACT

The advent of *Swift* has allowed, for the first time, the possibility to give Supergiant Fast X-ray Transients (SFXTs), the new class of High Mass X-ray Binaries discovered by INTEGRAL, non serendipitous attention throughout most phases of their life. In this paper we present our results based on the first year of intense *Swift* monitoring of four SFXTs, IGR J16479–4514, XTE J1739–302, IGR J17544–2619, and AX J1841.0–0536.

We obtain the first assessment of how long each source spends in each state using a systematic monitoring with a sensitive instrument. The duty-cycle of inactivity is $\sim 17, 28, 39, 55\%$ ($\sim 5\%$ uncertainty), for IGR J16479–4514, AX J1841.0–0536, XTE J1739–302, and IGR J17544–2619, respectively, so that true quiescence, which is below our detection ability even with the exposures we collected in one year, is a rare state, when compared with estimates from less sensitive instruments. This demonstrates that these transients accrete matter throughout their lifetime at different rates.

AX J1841.0–0536 is the only source which has not undergone a bright outburst during our monitoring campaign. Although individual sources behave somewhat differently, common X-ray characteristics of this class are emerging such as outburst lengths well in excess of hours, with a multiple peaked structure. A high dynamic range (including bright outbursts) of ~ 4 orders of magnitude have been observed in IGR J17544–2619 and XTE J1739–302, of ~ 3 in IGR J16479–4514, and of about 2 in AX J1841.0–0536 (this lowest range is due to the lack of bright flares). We also present a complete list of BAT on-board detections, which complements our previous work, and further confirms the continuous activity of these sources.

We performed out-of-outburst intensity-based spectroscopy. In particular, spectral fits with an absorbed blackbody always result in blackbody radii of a few hundred meters, consistent with being emitted from a small portion of the neutron star surface, very likely the neutron star polar caps.

We used the whole BAT dataset, since the beginning of the mission, to search for periodicities due to orbital motion and found $P_{\text{orb}} = 3.32$ d for IGR J16479–4514, confirming previous findings. We also present the UVOT data of these sources; we show the UVOT light curves of AX J1841.0–0536 and the ones of XTE J1739–302 before, during, and after the outbursts.

Key words: X-rays: binaries – X-rays: individual: IGR J16479–4514, XTE J1739–302, IGR J17544–2619, AX J1841.0–0536.

Facility: *Swift*

1 INTRODUCTION

Supergiant Fast X-ray Transients (SFXTs) are a sub-class of High Mass X-ray Binaries (HMXBs) recently discovered by INTEGRAL during the Galactic Plane monitoring (Sguera et al. 2005). They are firmly associated (via optical spectroscopy) with an O or B supergiant and display outbursts which are significantly shorter than typical Be/X-ray binaries, characterized by bright flares with a duration of a few hours and peak luminosities of 10^{36} – 10^{37} erg s $^{-1}$. The quiescence, characterized by a soft spectrum (likely thermal) and a low luminosity at $\sim 10^{32}$ erg s $^{-1}$ is a rarely-observed state (e.g. in’t Zand 2005). As their spectral properties resemble those of accreting pulsars, it is generally assumed that all members of the new class are HMXBs hosting a neutron star, although the only three SFXTs with a measured pulse period are AX J1841.0–0536 ($P_{\text{spin}} \sim 4.7$ s, Bamba et al. 2001), IGR J11215–5952 ($P_{\text{spin}} \sim 187$ s, Swank et al. 2007), and IGR J18483–0311 ($P_{\text{spin}} \sim 21$ s, Sguera et al. 2007). The mechanisms responsible for the observed short outbursts are still being debated. The proposed explanations (see Sidoli 2009, for a recent review) mainly involve the structure of the wind from the supergiant companion (in’t Zand 2005; Walter & Zurita Heras 2007; Negueruela et al. 2008; Sidoli et al. 2007), or the possible presence of gated mechanisms (see, Bozzo et al. 2008). The latter are due to the properties of the accreting neutron star (magnetar-like magnetic fields and slow pulse periods) which can halt the accretion for most of the time.

During February 2007, we monitored the outburst of the periodic SFXT IGR J11215–5952 (Romano et al. 2007; Sidoli et al. 2007) with *Swift* (Gehrels et al. 2004), in what became the most complete and deep set of X-ray observations of an outburst of a SFXT. Thanks to these observations, we discovered that the accretion phase during the bright outburst lasts much longer than a few hours. The orbital dependence of the accretion X-ray luminosity during the outburst led us to propose an alternative explanation for the outburst mechanism in IGR J11215–5952 (Sidoli et al. 2007), linked to the possible presence of a second wind component, in the form of a preferred plane for the outflowing wind from the supergiant donor. X-ray outbursts should be produced when the neutron star crosses this density enhanced wind component.

Following the success of the *Swift* observations on IGR J11215–5952, we extended the investigation to a small although well-defined sample of SFXTs. *Swift* was the most logical choice to monitor the light curves of our sample, because of its unique fast-slewing and flexible observing scheduling, which makes a monitoring effort cost-effective, its broad-band energy coverage that would allow us to model the observed spectra simultaneously in the 0.3–150 keV energy range, thus testing the prevailing models for accreting neutron stars, and the high sensitivity in the soft X-ray regime, where some of the SFXTs had never been observed.

In Sidoli et al. (2008, Paper I), we described the long-term X-ray emission outside the bright outbursts based on the first 4 months of data; in Romano et al. (2008c, Paper II) and Sidoli et al. (2009b, Paper III), we reported on the outbursts of IGR J16479–4514, and the prototypical IGR J17544–2619 and XTE J17391–302, respectively, while in Sidoli et al. (2009a, Paper IV) we report the results of more outbursts of XTE J1739–302 and IGR J17544–2619. In this paper we draw a general picture of our knowledge on SFXT, by summarizing the results on the outbursts caught by *Swift* during the first year of our ongoing campaign, and report on the XRT (Burrows et al. 2005) and UVOT (Romano et al. 2005) data col-

lected from 2007 October 26 to 2008 November 15, as well as the BAT (Barthelmy et al. 2005) data collected since the start of the mission. We also include data from the 2009 January 29 outburst of IGR J16479–4514 (Romano et al. 2009b).

2 OUR SAMPLE AND OBSERVATIONS

The four targets, IGR J16479–4514, XTE J1739–302, IGR J17544–2619, and AX J1841.0–0536 were selected by considering sources which, among several SFXT candidates, are confirmed SFXTs, i.e. they display both a ‘short’ transient (and recurrent) X-ray activity and they have been optically identified with supergiant companions [see Walter & Zurita Heras (2007) and references therein]. XTE J1739–302 and IGR J17544–2619, in particular, are generally considered prototypical SFXTs: XTE J1739–302 was the first transient which showed an unusual X-ray behavior (Smith et al. 1998), only recently optically associated with a blue supergiant (Negueruela et al. 2006). AX J1841.0–0536/IGR J18410–0535, was chosen because at the time it was the only SFXT, together with IGR J11215–5952, where a pulsar had been detected (Bamba et al. 2001). Finally, IGR J16479–4514 had displayed in the past a more frequent X-ray outburst occurrence than other SFXTs (see, e.g. Walter & Zurita Heras 2007), and offered an *a priori* better chance to be caught during an outburst.

For these sources we obtained 2–3 observations week $^{-1}$ object $^{-1}$, each 1 ks long with XRT in AUTO mode, to best exploit XRT automatic mode switching (Hill et al. 2004) in response to changes in the observed fluxes. This observing pace would naturally fit in the regular observation scheduling of γ -ray bursts (GRBs), which are the main observing targets for *Swift*. We also proposed for further target of opportunity (ToO) observations whenever one of the sources showed interesting activity, (such as indications of an imminent outburst) or underwent an outburst, thus obtaining a finer sampling of the light curves and allowing us to study all phases of the evolution of an outburst.

During the first year, we collected a total of 330 *Swift* observations as part of our program, for a total net XRT exposure of ~ 363 ks accumulated on all sources and distributed as shown in Table 1.

In this paper we also include the data on the 20 d campaign (for a total on-source time of ~ 34 ks) on IGR J16479–4514, which triggered the BAT on 2009 January 29 at 06:33:07 UT (image trigger=341452, Romano et al. 2009b). *Swift* slewed to the target so that the XRT started observing the field at 06:46:46.9 UT, 819.3 s after the BAT trigger. The BAT transient monitor showed enhanced emission (in excess of 20 mCrab) from 01:38:56 to 07:02:08 UT. During the image trigger interval (the 640 seconds starting at 2009-01-29 06:27:5) the rate was 0.022 ± 0.003 counts s $^{-1}$ (97 mCrab). IGR J16479–4514 showed renewed activity on 2009 February 8, starting from about 20:30 UT (La Parola et al. 2009). For the 504 s pointing starting at 2009-02-08 20:30 UT the BAT transient monitor rate was 0.019 ± 0.003 counts s $^{-1}$ (85 mCrab).

3 DATA REDUCTION

The XRT data were uniformly processed with standard procedures (XRTPIPELINE v0.11.6), filtering and screening criteria by using FTOOLS in the HEASOFT package (v.6.4). We considered both

Table 1. Summary of the *Swift*/XRT monitoring campaign of the four SFXTs during the first year.

Name	Campaign Start (yyyy-mm-dd)	Campaign End (yyyy-mm-dd)	N ^a	Exposure ^b (ks)	Outburst ^c Dates (yyyy-mm-dd)	BAT Trigger	References
IGR J16479–4514	2007-10-26	2008-10-25	70	75.2	2008-03-19 2008-05-21 <i>2009-01-29</i>	306829 312068 <i>341452</i>	Romano et al. (2008c) <i>Romano et al. (2009b); La Parola et al. (2009)</i>
XTE J1739–302	2007-10-27	2008-10-31	95	116.1	2008-04-08 2008-08-13 <i>2009-03-10</i>	308797 319963 <i>346069</i>	Sidoli et al. (2009b) Romano et al. (2008b), Sidoli et al. (2009a) <i>Romano et al. (2009a)</i>
IGR J17544–2619	2007-10-28	2008-10-31	77	74.8	2007-11-08 2008-03-31 2008-09-04 <i>2009-03-15</i>	308224	Krimm et al. (2007) Sidoli et al. (2009b) Romano et al. (2008a); Sidoli et al. (2009a) <i>Krimm et al. (2009)</i>
AX J1841.0–0536	2007-10-26	2008-11-15	88	96.5	none		
Total			330	362.6			

^a Number of observations obtained during the monitoring campaign.

^b *Swift*/XRT net exposure.

^c BAT trigger dates. We report the outburst that occurred in 2009 in italics, for the sake of completeness.

Table 2. Duty cycle of inactivity of the four SFXTs.

Name	Limiting Rate ^a (0.2–10 keV) (10 ^{−3} counts s ^{−1})	Limiting $F^{a,b}$ (2–10 keV) (10 ^{−12} erg cm ^{−2} s ^{−1})	Limiting $L^{a,b}$ (2–10 keV) (10 ³⁵ erg s ^{−1})	ΔT_{Σ} (ks)	P_{short} (%)	IDC (%)	Rate $_{\Delta T_{\Sigma}}$ (0.2–10 keV) (10 ^{−3} counts s ^{−1})
IGR J16479–4514	16	2.4	0.62	12.2	2	17	2.9 ± 0.7
XTE J1739–302	13	1.6	0.13	40.3	9	39	3.9 ± 0.4
IGR J17544–2619	13	1.2	0.17	37.0	10	55	1.9 ± 0.3
AX J1841.0–0536	13	1.7	0.45	26.6	3	28	2.4 ± 0.4

Count rates are in units of 10^{−3} counts s^{−1} in the 0.2–10 keV energy band. Observed fluxes and luminosities are in units of 10^{−12} erg cm^{−2} s^{−1} and 10³⁵ erg s^{−1} in the 2–10 keV energy band, respectively. ΔT_{Σ} is sum of the exposures accumulated in all observations, each in excess of 900 s, where only a 3- σ upper limit was achieved; P_{short} is the percentage of time lost to short observations; IDC is the *duty cycle of inactivity*, the time each source spends undetected down to a flux limit of 1–3 × 10^{−12} erg cm^{−2} s^{−1}; Rate $_{\Delta T_{\Sigma}}$ is detailed in the text (Sect. 4.1).

^a Based on a single 900 s exposure.

^b Based on the best fit model for the ‘low’ (or ‘medium’ if ‘low’ unavailable) absorbed power-law model in Table 4.

WT and PC data, and selected event grades 0–2 and 0–12, respectively (Burrows et al. 2005). When appropriate, we corrected for pile-up by determining the size of the point spread function (PSF) core affected by comparing the observed and nominal PSF (Vaughan et al. 2006), and excluding from the analysis all the events that fell within that region. We used the spectral redistribution matrices v010 in CALDB.

We retrieved the BAT orbit-by-orbit light curves (15–50 keV) covering the data range from February 12, 2005 to December 31, 2008 (MJD range 53413–54831) from the BAT Transient Monitor (Krimm et al. 2006, 2008) page¹.

The UVOT observed the 4 targets simultaneously with the XRT with the ‘Filter of the Day’, i.e. the filter chosen for all observations to be carried out during a specific day in order to minimize the filter wheel usage. The only exception are the observa-

tions during outbursts, when all filters were used in the typical GRB sequence (Roming et al. 2005). The data analysis was performed using the UVOTISUM and UVOTSOURCE tasks included in the FTOOLS software. The latter task calculates the magnitude through aperture photometry within a circular region and applies specific corrections due to the detector characteristics. The reported magnitudes are on the UVOT photometric system described in Poole et al. (2008), and are not corrected for Galactic extinction. At the position of IGR J16479–4514, no detection was achieved down to a limit of $u = 21.07$ mag. For IGR J17544–2619 only engineering data were collected, as is generally the case for a field which contains a source too bright to be observed; the only exceptions were the outburst segments 00308224000, and the two following it, 00035056021 and 00035056023 [see Table 7, and Sidoli et al. (2009b)], where we observe $v = 12.8$ mag and $uvw2 = 18.13 \pm 0.05$ and $uvw2 = 18.00 \pm 0.06$ mag, respectively.

All quoted uncertainties are given at 90 % confidence level

¹ <http://swift.gsfc.nasa.gov/docs/swift/results/transients/>

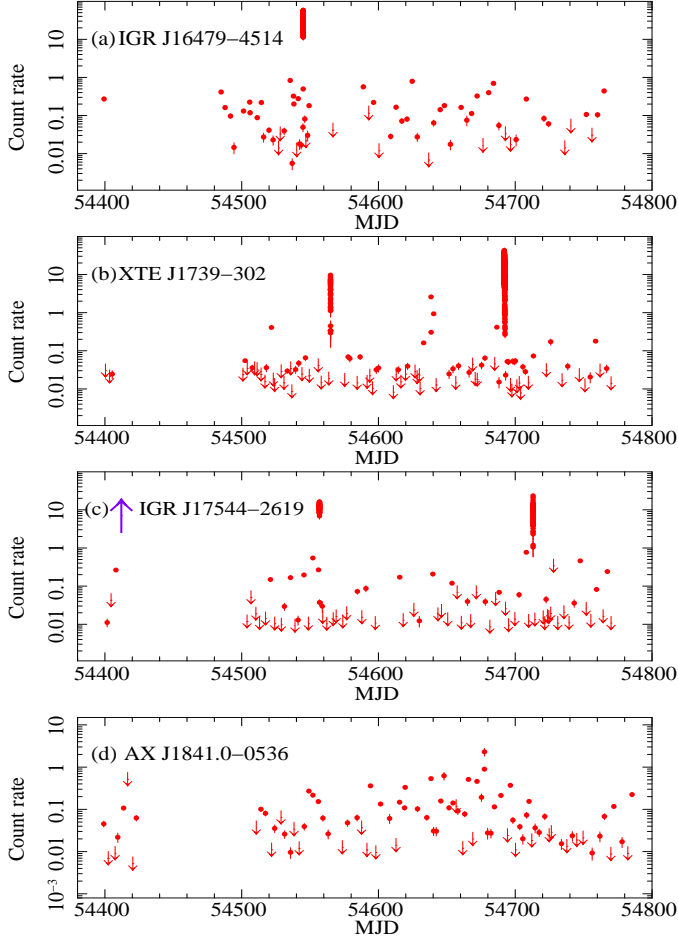


Figure 1. *Swift*/XRT (0.2–10 keV) light curves, corrected for pile-up, PSF losses, vignetting and background-subtracted. The data were collected from 2007 October 26 to 2008 November 15. The downward-pointing arrows are 3- σ upper limits. The upward pointing arrow marks an outburst that triggered the BAT on MJD 54,414, but which could not be followed by XRT because the source was Sun-constrained for the XRT.

for one interesting parameter unless otherwise stated. The spectral indices are parameterized as $F_\nu \propto \nu^{-\alpha}$, where F_ν (erg cm $^{-2}$ s $^{-1}$ Hz $^{-1}$) is the flux density as a function of frequency ν ; we adopt $\Gamma = \alpha + 1$ as the photon index, $N(E) \propto E^{-\Gamma}$ (ph cm $^{-2}$ s $^{-1}$ keV $^{-1}$).

4 TIMING

4.1 XRT Inactivity Duty Cycle

Fig. 1 shows the XRT light curves collected from 2007 October 26 to 2008 November 15, in the 0.2–10 keV band, which were corrected for pile-up, PSF losses, and vignetting, and background-subtracted. Each point in the light curves refers to the average flux observed during each observation performed with XRT; the exception are the outbursts (listed in Table 1) where the data were binned to include at least 20 source counts per time bin to best represent the count rate dynamical range. Due to the sources being

Sun-constrained between roughly 2007 December and 2008 January, depending on the target coordinates, no data were collected during those months.

Given the structure of the observing plan we can realistically consider our monitoring as a casual sampling of the light curve at a resolution of about ~ 4 d. Therefore, we can calculate the percentage of time each source spent in each relative flux state. In order to do this, we divided the observations into three states, namely *i*) BAT-detected outburst, *ii*) intermediate state (all observations yielding a firm detection excluding outburst ones), *iii*) ‘non detections’ (detections with a significance below 3σ). Since a few observations were interrupted by GRB events, the consequent non detection may be due to the short exposure, not exclusively to the source being faint. Therefore, to create a uniform subsample for the latter state, we excluded all observations that had a net exposure below 900 s. An exposure of 900 s corresponds to 2–10 keV flux limits that vary between 1 and 3×10^{-12} erg cm $^{-2}$ s $^{-1}$ (3σ), depending on the source. These values were derived from a measurement of the local background and a count rate to flux conversion calculated by using the best fit absorbed power-law models of the ‘low’ (or ‘medium’ if ‘low’ was not available) state in Table 4.

We define as *duty cycle of inactivity*, the time each source spends *undetected* down to a flux limit of $1\text{--}3 \times 10^{-12}$ erg cm $^{-2}$ s $^{-1}$,

$$\text{IDC} = \Delta T_\Sigma / [\Delta T_{\text{tot}} (1 - P_{\text{short}})],$$

where ΔT_Σ is sum of the exposures accumulated in all observations, each in excess of 900 s, where only a 3- σ upper limit was achieved (Table 2, column 5), ΔT_{tot} is the total exposure accumulated (Table 1, column 5), and P_{short} is the percentage of time lost to short observations (exposure < 900 s, Table 2, column 6). We obtain that $\text{IDC} \sim 17, 28, 39, 55\%$, for IGR J16479–4514, AX J1841.0–0536, XTE J1739–302, and IGR J17544–2619, respectively (Table 2, column 7). We estimate an error of $\sim 5\%$ on these values.

We accumulated all data for which no detections were obtained as single exposures (whose total exposure is ΔT_Σ), and performed a detection. The resulting cumulative mean count rate for each object is reported in Table 2 (column 8).

4.2 BAT on-board detections

In Table 3 we list the BAT on-board detections in the 15–50 keV band. If an alert was generated, a BAT trigger was assigned (cols. 4 and 8) and notices were disseminated². For some of these triggers a burst response (slew and repointing of the NFI) was also initiated, depending on GRB observing load, observing constraints, and interest in the sources. More details on several of these triggers can be found in the papers of our series (see Table 1, for references). These data show that the four sources are quite active even outside the outbursts, not only when observed by XRT, but also by BAT.

4.3 Searching for orbital periodicities in BAT data

We looked for evidence of orbital periodicities in the BAT data. We first considered the BAT data for the four sources binned orbit-by-orbit in the time range MJD 53413–54829. These data were further screened to exclude bad quality points (quality flag 1 and 2)

² <http://gcn.gsfc.nasa.gov/gcn/swift-grbs.html>

Table 3. BAT on-board detections in the 15–50 keV band.

MJD	Date	Time ^a	BAT Trigger N. ^b	S/N ^c	MJD	Date	Time ^a	BAT Trigger N. ^b	S/N ^c
IGR J16479–4514					XTE J1739–302				
53612	2005-08-30	04:03:28–04:13:52	152652 (NFI)	7.71	53581	2005-07-30	00:23:12–00:28:56		
53811	2006-03-17	08:03:51			53663	2005-10-20	12:53:04		
53875	2006-05-20	17:32:39–17:35:51	210886 (no slew)	5.78	53765	2006-01-30	18:33:43–20:26:15		
53898	2006-06-12	06:58:31			53798	2006-03-04	04:52:31		
53910	2006-06-24	20:19:59	215914 (no slew)	5.34	53806	2006-03-12	07:13:27		
54095	2006-12-26	22:39:43–22:45:03			54140	2007-02-09	17:33:03–17:34:07		
54167	2007-03-08	06:04:55			54161	2007-03-02	13:39:11–15:05:27	^d	
54196	2007-04-06	15:22:55			54168	2007-03-09	11:09:51–11:14:47	^d	
54239	2007-05-19	19:53:59–20:04:39			54269	2007-06-18	03:09:43–03:10:47	282535 (no slew)	6.53
54310	2007-07-29	12:07:35	286412 (no slew)	9.98	54411	2007-11-07	04:38:15–04:42:31		
54320	2007-08-08	21:13:51			54564	2008-04-08	16:43:19–21:28:15	308797 (NFI)	7.83
54368	2007-09-25	18:14:31			54565	2008-04-09	00:45:11–00:51:35		
54506	2008-02-10	05:35:43			54632	2008-06-15	06:56:39		
54535	2008-03-10	13:11:03–13:20:39			54673	2008-07-26	14:13:27		
54544	2008-03-19	22:44:47–22:59:59	306829 (NFI)	12.02 ^e	54691	2008-08-13	23:49:19–23:51:27	319963 (NFI)	9.15
54572	2008-04-16	17:07:11			54692	2008-08-14	00:04:23–03:06:39	319964 (NFI)	11.14
54607	2008-05-21	06:03:43–15:38:23	312068 (no slew)	7.21	54724	2008-09-15	12:59:59–13:06:23		
54664	2008-07-17	18:10:15			54900	2009-03-10	18:18:38–18:39:58	346069 (NFI)	6.81
54679	2008-08-01	03:38:31–03:49:03							
54682	2008-08-04	04:06:55–04:14:39							
54687	2008-08-09	01:11:51							
54826	2008-12-26	15:55:11–15:57:19							
54860	2009-01-29	06:32:06–06:48:14	341452 (NFI)	10.68					
IGR J17544–2619					AX J1841.0–0536				
53996	2006-09-18	09:07:43			53821	2006-03-27	00:51:03–08:39:27	202892 (no slew)	5.45
53998	2006-09-20	11:11:43	^f		53834	2006-04-09	16:33:43		
54009	2006-10-01	10:34:47			53845	2006-04-20	14:42:31		
54035	2006-10-27	00:33:11			54026	2006-10-18	10:50:23		
54372	2007-09-29	13:21:51–16:36:55			54053	2006-11-14	10:21:19		
54387	2007-10-14	00:39:35–19:57:27			54139	2007-02-08	22:21:59		
54412	2007-11-08	01:31:03–06:16:47			54195	2007-04-05	12:00:31		
54556	2008-03-31	20:50:47	308224 (NFI)	9.10					
54565	2008-04-09	18:17:19							
54611	2008-05-25	14:43:51–14:55:03							

^a Time of the start of the BAT trigger, or the time range when on-board detections were obtained.

^b BAT regular trigger, as was disseminated through GCNs. NFI indicates that there are data from the narrow-field instrument; no slew, indicates that *Swift* did not slew to the target.

^c On-board image significance in units of σ .

^d Also reported by Blay et al. (2008).

^e Trigger 306830 had S/N = 21.64, see Romano et al. (2008c).

^f Also reported by Ducci et al. (2008).

and referred to the solar system barycenter (SSB) by using the task EARTH2SUN.

A folding technique was applied to the baricentered arrival times by searching in the 0.1–50 d period range and by building 16-bin pulse profiles with a step given by $P^2/(N \Delta T)$, where N is the number of phase bins, and ΔT is the data span length. We find significant evidence for orbital modulation for IGR J16479–4514 with a best period of 286792 ± 42 s ($P_{\text{orb}} = 3.3193 \pm 0.0005$ days) referred to the epoch time MJD 54170.20500213, with a χ^2 value of 155.8. As shown in the periodogram in Fig. 2a, this periodicity stands out from the noise and is certainly not due to the satellite orbital period or its multiples, as instead is the case for the peaks appearing below 1 day. Peaks at periods higher than 5 days are mul-

tiples of the P_{orb} . A zoomed-in region of the periodogram around the candidate P_{orb} is shown in Fig. 2b. The statistics of the data is not Gaussian, so assessment of the significance of this periodicity needs to be performed on the noise distribution of χ^2 in the periodogram. Fig. 2c represents the noise distribution of the powers of the periodogram after removal of the satellite orbital data period (and its multiples), and of the multiples of P_{orb} . In order to evaluate the significance of the signal at P_{orb} , we fit the distribution for $25 < \chi^2 < 80$ with an exponential function and evaluated the integral of the best-fit function beyond the value of the χ^2 obtained at P_{orb} . This integral yields a number of chance occurrences due to noise of 1.24×10^{-5} , corresponding to 4.5 standard deviations in Gaussian statistics. In Fig. 2d we show the pulsed profile folded

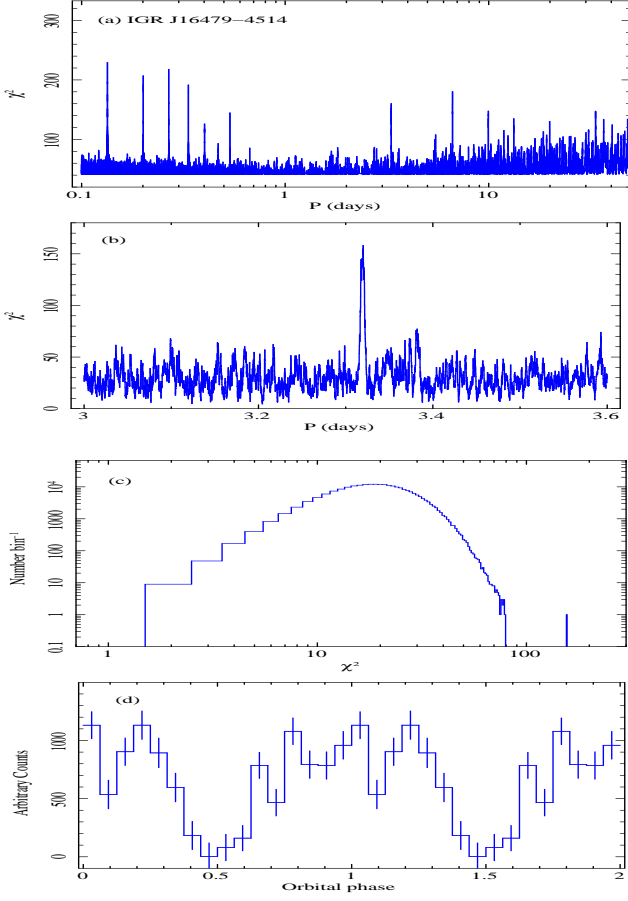


Figure 2. (a): Periodogram of *Swift*/BAT (15–50 keV) data for IGR J16479–4514 (MJD range 53413–54829) from the BAT Transient Monitor in the whole time range examined. (b): Close-up around the $P = 3.32$ day periodicity. (c): Distribution of χ^2 values. (d): Light curve folded at a period $P = 3.32$ day, with 16 phase bins.

at P_{orb} . There is clear evidence for an eclipse phase, whose epoch centroid, evaluated by fitting the data around the dip with a Gaussian function, is MJD 54171.11 \pm 0.05. This confirms the results of Jain et al. (2009).

Adopting the same techniques for XTE J1739–302 (Fig. 3a) we find marginal evidence for a signal above the noise at 1111605.1 \pm 631.3 s ($P_{\text{orb}} = 12.8658 \pm 0.0073$ days) with a χ^2 value of 94.7. The second highest peak in Fig. 3a is the first multiple of P_{orb} . The chance probability to obtain this signal at P_{orb} is 3.1×10^{-2} , corresponding to 2.1 standard deviations in Gaussian statistics. By repeating this kind of analysis on 1/4, 1/2, 3/4 and the whole BAT data sample, we verified that the power at this P_{orb} increases with time baseline, as is expected of signal, as opposed to noise. This strengthens the possibility that this is a true periodicity.

No significant evidence for orbital periodicity was found for either IGR J17544–2619 or AX J1841.0–0536.

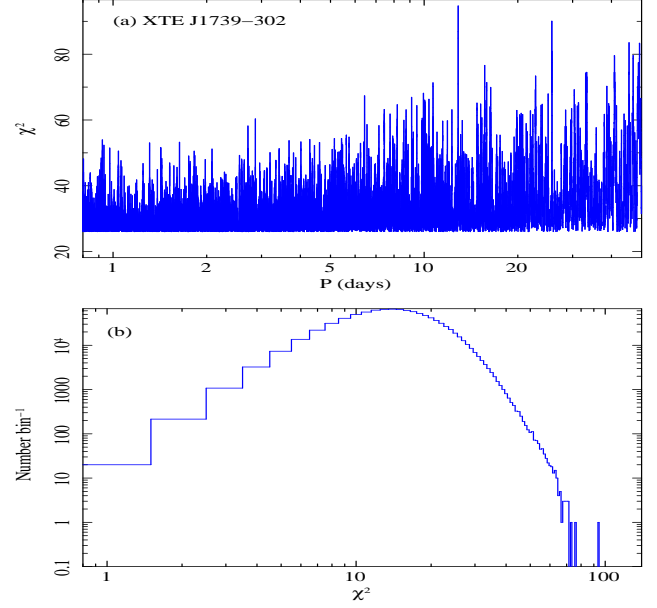


Figure 3. (a): Periodogram of *Swift*/BAT (15–50 keV) data for XTE J1739–302 (MJD range 53413–54829) from the BAT Transient Monitor in the whole time range examined. (b): Distribution of χ^2 values.

4.4 Searching for spin periodicities in XRT data

We also looked for evidence of spin periodicities in XRT data. For each source, we performed a timing analysis to search for coherent pulsations within *each single observation* with a slow Fourier analysis on the fundamental harmonics in the 0.0047–0.199418 Hz frequency range (the latter being the Nyquist frequency of the data set, corresponding to a period of 5.01460 s), with the frequency resolution $df = 1/(2\Delta T)$ Hz, where ΔT is the length of each observation. As the expected power of the pulsed emission is $P_i = K \times F_P^2 \times N_t + 2$, we only used observations with a minimum statistic content $N_t > 300$ counts, that would yield a detection with a significance greater than 3 standard deviations for a signal with a pulsed fraction of $F_P = 0.2$, and $K = 0.5$ (sinusoidal profile). No significant deviations from a statistically flat distribution was revealed in the Fourier spectra of these observations.

In order to reveal the presence of a pulsed signal that could be undetectable in single observations because of the poor statistics, we performed a *stacked timing analysis* on a larger set of observations. This analysis consists in summing the power spectra obtained from single observations with a common frequency range (0.005–0.2 Hz) and resolution $1/2\Delta T_{\text{max}}$, where ΔT_{max} is the elapsed time of the longest observation. The averaged power spectrum will have a distribution with mean 2 and standard deviation $2/\sqrt{N}$, where N is the number of summed power spectra. However, we cannot add arbitrarily long amounts of data without taking into account the Doppler modulation due to orbital motion which could destroy the coherence of the pulsed signal. For IGR J16479–4514, for which a firm detection of a P_{orb} was obtained, we could minimize the effect of the orbital Doppler modulation, by summing the spectra which are close in orbital phase. Under the simplifying assumption of a circular orbit, we evaluated the orbital phase for each XRT observation and divided the sample in 4 phase intervals: 0.85–0.15, 0.15–0.35, 0.35–0.65, 0.65–0.85. The different ampli-

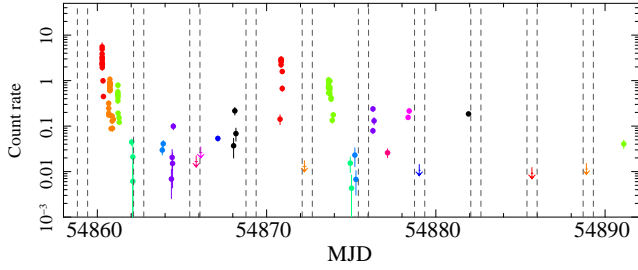


Figure 4. XRT light curve of the *Swift*/XRT observations after the 2009 January 29 outburst of IGR J16479–4514 in the 0.3–10 keV band, background-subtracted and corrected for pile-up, PSF losses, and vignetting. Different colours denote different observations. Filled circles are full detections ($S/N > 7$), while downward-pointing arrows are 3- σ upper limits. The vertical lines mark the predicted positions of the eclipse.

tudes were chosen to take into account the different values of the tangential velocity of the compact object along its orbit. In the four stacked spectra we found no evidence for a significant excess above the noise distribution.

4.5 Searching for eclipses in IGR J16479–4514 XRT data

The data of the whole XRT campaign on IGR J16479–4514 were sought for the presence of eclipses, suggested by Bozzo et al. (2008) on the basis of the analysis of an XMM-Newton observation. We created event lists for the whole campaign and selected those inside and outside the eclipses, where by ‘inside the eclipse’ we consider the time interval between the start of the eclipse as defined by Bozzo et al. (2008) and 0.6 d later [using the ephemeris from (Jain et al. 2009)]. We then calculated the net (subtracted for scaled background) count rate in the two cases. We obtain $(6 \pm 1) \times 10^{-3}$ counts s^{-1} (inside) and 0.169 ± 0.002 counts s^{-1} (outside). Consistent values [$(6 \pm 3) \times 10^{-3}$ and 0.203 ± 0.003 counts s^{-1} , respectively] are measured during the 2009 January outburst. This indicates that the source is in two distinct flux levels inside and outside the predicted times of the eclipses at the $\sim 50\sigma$ level. We also calculated the count rates within individual time slices inside eclipses and find that they never exceed 0.013 counts s^{-1} . We can thus conclude that the XRT data are consistent with the presence of an eclipse on the longest baseline so far examined. In particular, Fig. 4 shows the light curve of IGR J16479–4514 during the 2009 January 29 outburst with vertical lines marking the predicted positions of the eclipse times.

4.6 UVOT light curves

We report for the first time on optical/UV observations performed with UVOT simultaneously to our *Swift*/XRT monitoring of the SFXTs. In Fig. 5a and 5b we show the UVOT *u* and *uvw1* light curves of XTE J1739–302 of the whole campaign. The dashed vertical lines mark the two X-ray outbursts (2008 April 8, 2008 August 13; Fig. 5b). The ultraviolet filters only registered upper limits for this source during the outbursts. We consider the correspondence between the X-ray peak and the *u* magnitude. During the first outburst the *u* band shows an increase of ~ 0.9 mag with respect to the campaign mean or a factor of ~ 2.5 in flux. Depending on the choice of background regions this is a 2–3 σ effect. During the second outburst the *u* magnitude is consistent with the mean for the whole campaign; the *b* and *v* magnitudes, collected as part of the

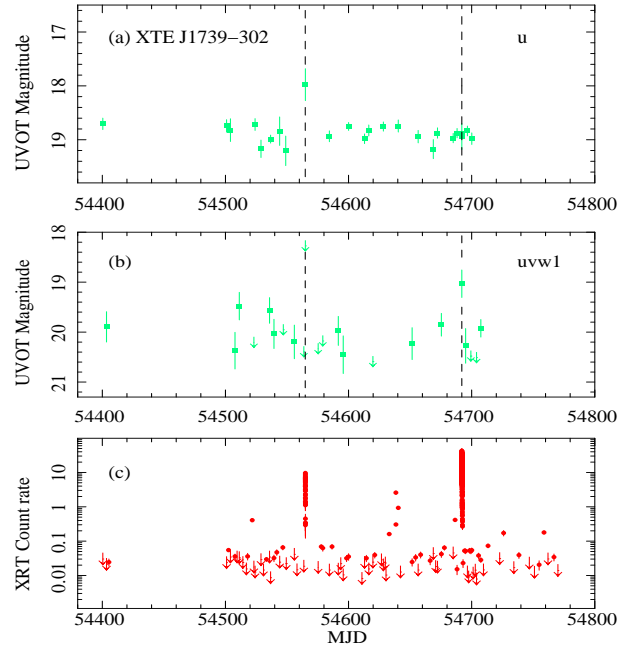


Figure 5. Light curves of XTE J1739–302. (a) *Swift*/UVOT *u* light curve; (b) *Swift*/UVOT *uvw1* light curve; (c) *Swift*/XRT light curve. The vertical dashed lines mark the BAT outbursts.

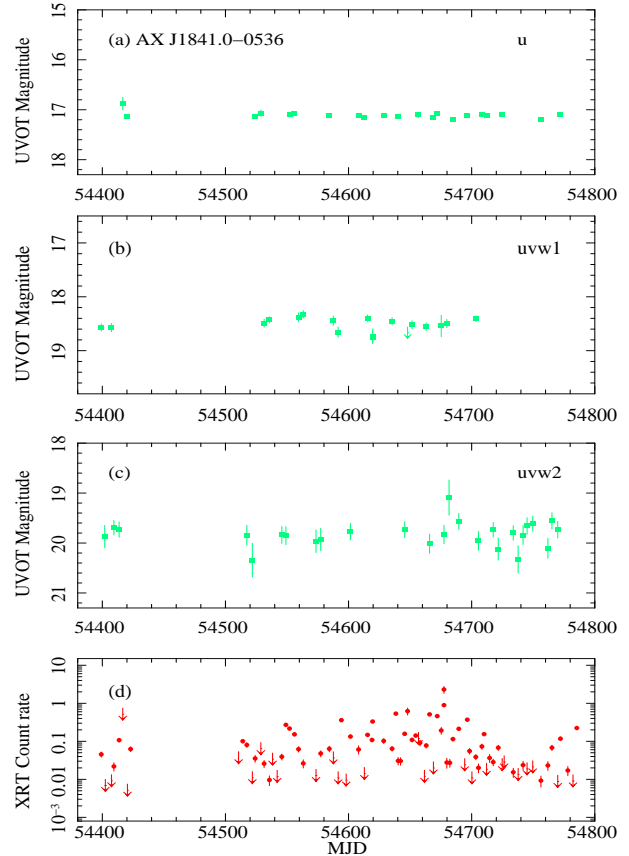


Figure 6. Light curves of AX J1841.0–0536. (a) *Swift*/UVOT *u* magnitudes; (b) *Swift*/UVOT *uvw1* magnitudes; (c) *Swift*/XRT *uvw2* magnitudes. (d) *Swift*/XRT light curve.

GRB-chasing filter scheme, show the same level as in the first one. The *uvw1* magnitudes show a larger degree of variability when compared with the *u* band. We also investigated intra-day variability during the outbursts, but found no significant variation within the errors in all bands.

In Fig. 6a,b,c we show the UVOT *u* and *uvw1*, and *uvw2* light curves of AX J1841.0–0536. The *u* and *uvw1* are remarkably stable, while the *uvw2* show some degree of variability. We note that the highest point in the *uvw2* light curve is not simultaneous with the X-ray peak.

5 X-RAY SPECTROSCOPY

5.1 The 2009 January 29 outburst of IGR J16479–4514

In response to the 2009 January 29 outburst of IGR J16479–4514, *Swift* performed a delayed slew, so that the NFI were on target > 800 s after the trigger (Romano et al. 2009b). At this point, the flux registered by the BAT was rather low, and meaningful broad-band (XRT+BAT) spectroscopy is not possible, given the 107 s overlap in the observations. Therefore, here we only report the fits to the XRT data. An absorbed power-law model yielded an absorbing column of $N_{\text{H}} = (7.1^{+2.6}_{-2.0}) \times 10^{22} \text{ cm}^{-2}$, a photon index $\Gamma = 1.63^{+0.53}_{-0.46}$, and an unabsorbed flux in the 2–10 keV band is $2 \times 10^{-10} \text{ erg cm}^{-2} \text{ s}^{-1}$. The X-ray spectrum extracted from segment 00030296087, when the source showed rebrightening (La Parola et al. 2009), was also fit with an absorbed power-law model, obtaining $\Gamma = 1.29^{+0.53}_{-0.46}$, $N_{\text{H}} = (7.1^{+2.6}_{-2.0}) \times 10^{22} \text{ cm}^{-2}$, and unabsorbed flux in the 2–10 keV band of $3 \times 10^{-10} \text{ erg cm}^{-2} \text{ s}^{-1}$. These results are generally consistent with the ones found in Romano et al. (2008c), which describes the outburst of this source which occurred on 2008 March 19, 315 days earlier. We also note that, as found in Romano et al. (2008c), the derived N_{H} is in excess of the one along the line of sight, $1.87 \times 10^{22} \text{ cm}^{-2}$. The broad-band spectroscopy of the other outbursts caught during the campaign has already been reported on elsewhere [Romano et al. (2008c); Sidoli et al. (2009a,b); see Table 1] and we will also summarize them below.

5.2 Out-of-outburst X-ray spectroscopy

In the remainder of this section we concentrate on the out-of-outburst emission. To characterize the spectral properties of the sources in several states, we accumulated the events in each observation when the source was not in outburst and a detection was achieved. For these events we estimated from the light curves (binned at a 100 s resolution) three count rate levels, CR_1 , CR_2 , and CR_3 (reported in Table 4) that would yield comparable statistics (and at least 1600 counts) in the ranges $CR_1 < CR < CR_2$ (low), $CR_2 < CR < CR_3$ (medium), and $CR > CR_3$ (high). If the statistics did not allow this, then we only considered two intensity levels (high and medium). Exposure maps were created for each of these intensity-selected event files. We then combined the intensity-selected event files (and their exposure maps) and extracted a single spectrum for each source by integrating over all the available observing time within these intensity limits. Ancillary response files were generated with XRTMKARF, and they account for different extraction regions, vignetting, and PSF corrections. The spectra were rebinned with a minimum of 20 counts per energy bin to allow χ^2 fitting. Each spectrum was fit in the energy range

0.3–10 keV with a single absorbed power law, or an absorbed black body.

We also extracted spectra from the event list accumulated from all observations for which no detections were obtained as single exposures (very low). These spectra consisted of ~ 100 counts each, so Cash (Cash 1979) statistics and spectrally unbinned data were used, instead. When fitting with free parameters, the best fit value for N_{H} turned out to be consistent with 0, i.e., well below the column derived from optical spectroscopy. In this case, we performed further fits by adopting as lower limit on the absorbing column the value derived from the Galactic extinction estimate along the line of sight to each source from Rahoui et al. (2008), with a conversion into Hydrogen column, $N_{\text{H}} = 1.79 \times 10^{21} A_V \text{ cm}^2$ (Predehl & Schmitt 1995). As a comparison, we also report the simple hardness ratios.

The spectra and contour plots of photon index vs. column density are shown in Fig. 7 and 8, respectively, while the spectral parameters are reported in Table 4, where we also report the average 2–10 keV luminosities calculated by adopting distances determined by Rahoui et al. (2008) from optical spectroscopy of the supergiant companions (4.9 kpc for IGR J16479–4514, 2.7 kpc for XTE J1739–302, and 3.6 kpc for IGR J17544–2619). For AX J1841.0–0536 two estimates of the distance are available, Nespola et al. (2008, $3.2^{+2.0}_{-1.5}$ kpc) and Sguera et al. (2009, 6.9 ± 1.7 kpc), and we assumed a distance of 5 kpc, which is consistent with both.

We note that spectral fits with an absorbed blackbody always result in blackbody radii of a few hundred meters (at the source distances, see Table 4, and Fig. 9), consistent with being emitted from a small portion of the neutron star surface, very likely the neutron star polar caps (Hickox et al. 2004). Indeed, since SFXTs are wind accretors, alternative origins for the small emitting region, such as small hot regions in an accretion disk, can be discarded.

6 DISCUSSION

We report on the results of an entire year of monitoring campaign with *Swift* of a sub-sample of SFXTs. For the first time it is possible to investigate in depth the long-term properties of this new class of puzzling X-ray transients, assessing the characteristics of three different source states: the bright outbursts, the intermediate intensity state, and the quiescence.

During this first year of monitoring, we have obtained multi-wavelength observations of 5 outbursts of 3 different sources (see Table 1). As reported in Romano et al. (2008c); Sidoli et al. (2009a,b), we studied the broad-band simultaneous spectra (0.3–150 keV) of three SFXTs. They can be fit with models traditionally adopted for accreting X-ray pulsars (absorbed cutoff power laws), even in the objects where proof of the presence of a neutron star (as derived from a spin period) is still unavailable. Considerable differences can be found in the behaviour of the absorbing column among the examined cases, and the new data from the 2009 January 29 outburst of IGR J16479–4514 fit well in this picture.

Our *Swift* monitoring campaign has demonstrated for the first time that X-ray emission from SFXTs is still present outside the bright outbursts, although at a much lower level (10^{33} – $10^{34} \text{ erg s}^{-1}$). This was already emerging from the first four months of this campaign (Sidoli et al. 2008), but now we have accumulated enough statistics to allow intensity selected spectroscopy of the out-of-outburst emission. Spectral fits performed adopting simple models, such as an absorbed power law or a blackbody (more

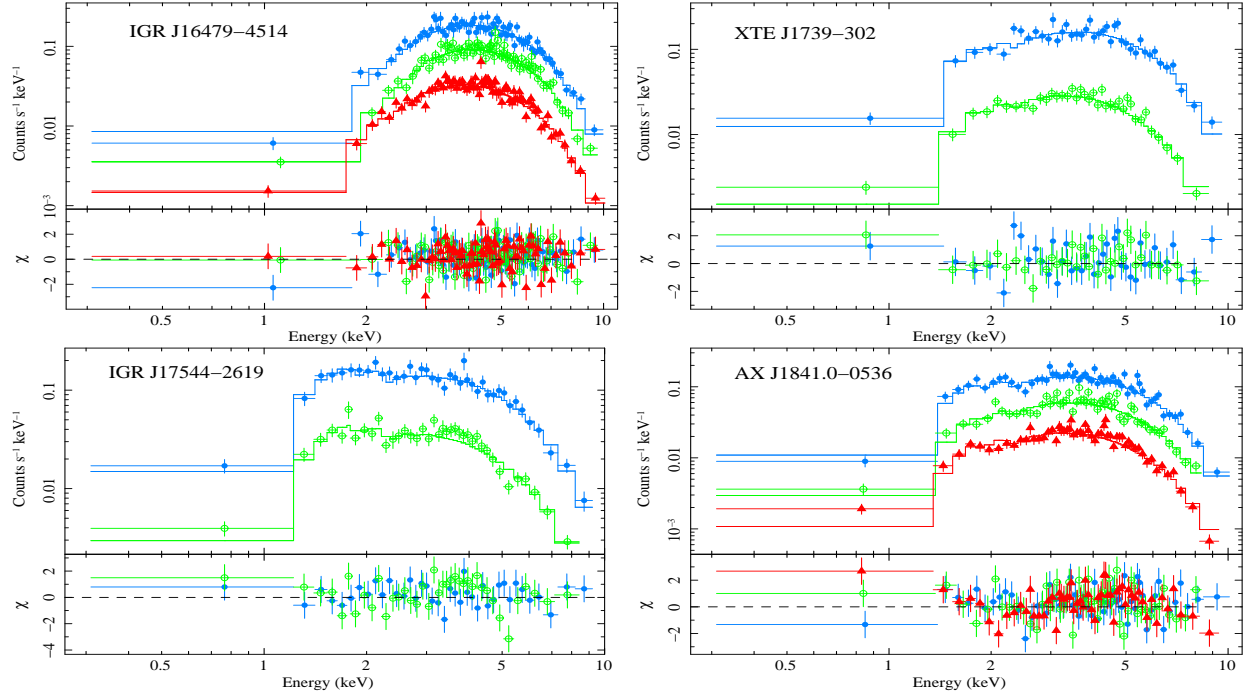


Figure 7. Spectroscopy of the 2007–2008 observing campaign. Upper panels: XRT/PC data fit with an absorbed power law. Lower panels: the residuals of the fit (in units of standard deviations). Filled blue circles, green empty circles, and red filled triangles mark high, medium, and low states, respectively.

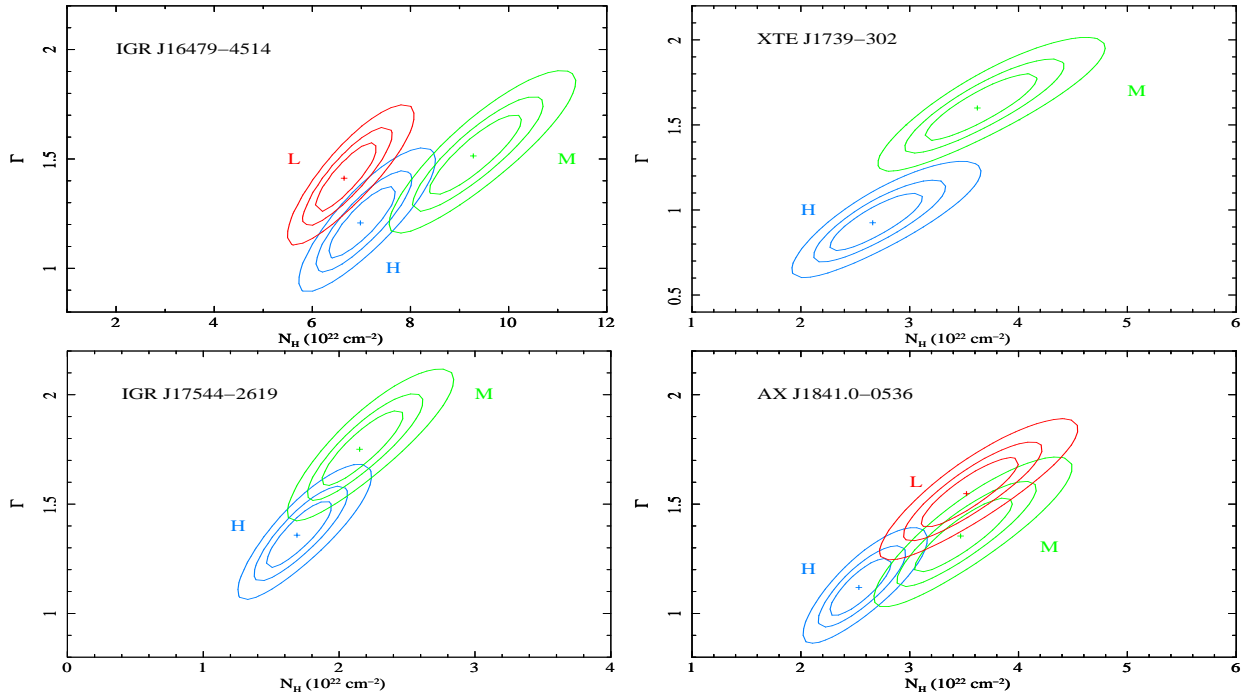


Figure 8. XRT time selected spectroscopy. The $\Delta\chi^2 = 2.3, 4.61$ and 9.21 contour levels for the column density in units of 10^{22} cm^{-2} vs. the photon index, with best fits indicated by crosses. The color scheme is the same as in Fig. 7. The labels L, M, and H mark low, medium, and high states, respectively.

Table 4. XRT spectroscopy of the four SFXTs (2007+2008 data set).

Name	Spectrum	Rate (counts s ⁻¹)	N_{H} (10 ²² cm ⁻²)	parameter Γ	Hardness ^a Ratio	Flux ^b (2–10 keV)	Luminosity ^c (2–10 keV)	$\chi^2_{\text{red}}/\text{dof}^{\text{d}}$ Cstat(%)
IGR J16479–4514	high	>0.52	7.0 ^{+0.8} _{-0.7}	1.2 ^{+0.2} _{-0.2}		120	5	1.1/131
	medium	[0.25–0.52]	9.3 ^{+1.1} _{-1.0}	1.5 ^{+0.2} _{-0.2}		54	3	1.0/132
	low	[0.06–0.25]	6.7 ^{+0.7} _{-0.7}	1.4 ^{+0.2} _{-0.2}		19	0.8	0.9/144
	very low ^e	<0.06	3.3 ^{+1.4} _{-0.0}	1.5 ^{+0.5} _{-0.4}		1.8	0.04	482.3(89.3)
	very low ^f	<0.06	0.3 ^{+0.6} _{-0.3}	0.3 ^{+0.5} _{-0.4}	0.9 ± 0.3	1.8	0.05	471.5(50.2)
XTE J1739–302	high	>0.33	2.7 ^{+0.5} _{-0.4}	0.9 ^{+0.2} _{-0.2}		120	1	1.1/77
	medium	[0.07–0.33]	3.6 ^{+0.6} _{-0.5}	1.6 ^{+0.2} _{-0.2}		15	0.2	0.9/73
	very low ^e	<0.07	1.7 ^{+0.2} _{-0.0}	1.3 ^{+0.3} _{-0.3}		0.5	0.005	614.3(96.3)
	very low ^f	<0.07	0.3 ^{+0.3} _{-0.2}	0.5 ^{+0.3} _{-0.3}	0.6 ± 0.3	0.6	0.006	598.9(64.7)
IGR J17544–2619	high	>0.33	1.7 ^{+0.3} _{-0.3}	1.4 ^{+0.2} _{-0.2}		62	1	0.9/75
	medium	[0.07–0.33]	2.1 ^{+0.3} _{-0.3}	1.8 ^{+0.2} _{-0.2}		14	0.3	1.0/72
	very low ^e	<0.07	1.1 ^{+0.1} _{-0.0}	2.2 ^{+0.3} _{-0.4}		0.2	0.002	381.8(83.0)
	very low ^f	<0.07	0.4 ^{+0.3} _{-0.3}	1.4 ^{+0.5} _{-0.4}	0.2 ± 0.3	0.2	0.003	372.0(53.1)
AX J1841.0–0536	high	>0.4	2.5 ^{+0.3} _{-0.3}	1.1 ^{+0.1} _{-0.1}		80	3	1.2/110
	medium	[0.18–0.4]	3.5 ^{+0.5} _{-0.5}	1.3 ^{+0.2} _{-0.2}		34	1	1.1/102
	low	[0.05–0.18]	3.5 ^{+0.5} _{-0.3}	1.5 ^{+0.2} _{-0.2}		11	0.4	1.2/104
	very low ^e	<0.05	0.3 ^{+0.3} _{-0.3}	0.6 ^{+0.4} _{-0.4}	1.3 ± 1.0	0.6	0.02	449.5(54.7)
Absorbed blackbody				kT_{bb}	Radius (km)			
IGR J16479–4514	high	>0.52	4.2 ^{+0.5} _{-0.5}	1.9 ^{+0.1} _{-0.1}	0.54 ^{+0.06} _{-0.05}	110	4	1.2/131
	medium	[0.25–0.52]	5.7 ^{+0.7} _{-0.6}	1.8 ^{+0.1} _{-0.1}	0.43 ^{+0.05} _{-0.04}	51	2	1.1/132
	low	[0.06–0.25]	3.8 ^{+0.5} _{-0.4}	1.8 ^{+0.1} _{-0.1}	0.25 ^{+0.03} _{-0.02}	17	0.6	1.0/144
	very low ^e	<0.06	3.3 ^{+0.5} _{-0.0}	1.2 ^{+0.2} _{-0.2}	0.14 ^{+0.05} _{-0.03}	1.3	0.04	486.8(99.5)
	very low ^f	<0.06	0.04 ^{+0.37} _{-0.04}	1.9 ^{+0.5} _{-0.4}	0.054 ^{+0.022} _{-0.001}	1.4	0.04	462.4(67.3)
XTE J1739–302	high	>0.33	1.3 ^{+0.3} _{-0.2}	1.9 ^{+0.2} _{-0.1}	0.28 ^{+0.04} _{-0.03}	100	1	1.3/77
	medium	[0.07–0.33]	1.5 ^{+0.3} _{-0.3}	1.5 ^{+0.1} _{-0.1}	0.16 ^{+0.02} _{-0.02}	13	0.1	0.8/73
	very low ^e	<0.07	1.7 ^{+0.1} _{-0.0}	1.3 ^{+0.2} _{-0.1}	0.04 ^{+0.01} _{-0.01}	0.5	0.004	646.1(100.0)
	very low ^f	<0.07	0.0 ^{+0.1} _{-0.0}	1.7 ^{+0.3} _{-0.2}	0.022 ^{+0.005} _{-0.004}	0.5	0.004	597.8(49.8)
IGR J17544–2619	high	>0.33	0.6 ^{+0.1} _{-0.1}	1.4 ^{+0.1} _{-0.1}	0.44 ^{+0.05} _{-0.04}	53	0.9	1.3/75
	medium	[0.07–0.33]	0.8 ^{+0.2} _{-0.2}	1.2 ^{+0.1} _{-0.1}	0.30 ^{+0.04} _{-0.03}	12	0.2	1.1/72
	very low ^e	<0.07	1.1 ^{+0.1} _{-0.0}	0.8 ^{+0.1} _{-0.1}	0.08 ^{+0.03} _{-0.02}	0.2	0.002	425.9(99.9)
	very low ^f	<0.07	0.0 ^{+0.1} _{-0.0}	1.1 ^{+0.2} _{-0.1}	0.04 ^{+0.01} _{-0.01}	0.2	0.002	381.8(50.5)
AX J1841.0–0536	high	>0.4	1.2 ^{+0.2} _{-0.2}	1.7 ^{+0.1} _{-0.1}	0.51 ^{+0.05} _{-0.05}	71	2	1.5/110
	medium	[0.18–0.4]	1.7 ^{+0.3} _{-0.3}	1.6 ^{+0.1} _{-0.1}	0.39 ^{+0.03} _{-0.03}	30	1	1.2/102
	low	[0.05–0.18]	1.5 ^{+0.3} _{-0.2}	1.5 ^{+0.1} _{-0.1}	0.24 ^{+0.03} _{-0.02}	9.9	0.3	1.0/104
	very low ^e	<0.05	0.0 ^{+0.1} _{-0.0}	1.7 ^{+0.4} _{-0.3}	0.04 ^{+0.01} _{-0.01}	0.5	0.02	451.7(50.0)

^a Hardness ratio 4–10 keV / 0.2–4 keV .^b Average observed 2–10 keV fluxes in units of 10⁻¹² erg cm⁻² s⁻¹ .^c Average 2–10 keV X-ray luminosities in units of 10³⁵ erg s⁻¹ calculated adopting distances determined by Rahoui et al. (2008).^d Reduced χ^2 and dof, or Cash statistics Cstat and percentage of realizations (10⁴ trials) with statistic > Cstat.^e Fit performed with constrained column density (see Sect 5.2).^f Fit performed with free column density (see Sect 5.2).

complex models were not required by the data) result in hard power law photon indices (always in the range $\Gamma \sim 0.8$ –2) or in hot black bodies ($kT_{\text{BB}} \sim 1$ –2 keV). It is remarkable that the statistics now accumulated allow us to constrain well the spectral parameters of the intermediate level of X-ray emission: in particular, when a black-body model is adopted, the resulting radii of the emitter for all 4 SFXTs (and all the intensity states) is *always only* a few hundred

meters (note that even with several kpc of uncertainty in the distance determination, the emitting regions are always significantly smaller than the neutron star radius). This is clearly indicative of an emitting region which is only a fraction of the neutron star surface, and can be associated in a natural way with the polar caps of the neutron star, (Hickox et al. 2004). This evidence, coupled with the high level of flux variability and hard X-ray spectra, strongly

supports the fact that the intermediate and low intensity level of SFXTs is produced by the accretion of matter onto the neutron star, demonstrating that SFXTs are sources which do not spend most of their lifetime in quiescence. This observational evidence rules out all models for the SFXTs emission which predict that the SFXTs are in quiescence when they are not in outburst (e.g., Bozzo et al. 2008). Even the accumulation of matter onto the neutron star magnetosphere is very difficult to reconcile with our determination of the emitting radius, which is always smaller than 1 km.

After following the X-ray light curves of the four SFXTs for one year, we have obtained the first assessment of how long each source in our sample spends in each state using a systematic monitoring. The duty-cycle of inactivity is $\sim 17, 28, 39, 55\%$ (5% uncertainty), for IGR J16479–4514 AX J1841.0–0536, XTE J1739–302, and IGR J17544–2619, respectively. For IGR J16479–4514 a contribution to the time spent in inactivity is due to the X-ray eclipses, hence the above 17% is in fact an upper limit to the true quiescent time. In the latter three SFXTs this inactivity duty cycle, where the sources are undetected with *Swift*, can be associated with the true quiescence (that is, no accretion) and/or with an accretion at a very low rate. Thus, the quiescence in these transients is a rare state.

The lowest luminosity level we could monitor (‘very low’ intensity level in Table 4) with *Swift* is reached in XTE J1739–302 ($6 \times 10^{32} \text{ erg s}^{-1}$, 2–10 keV) and in IGR J17544–2619 ($3 \times 10^{32} \text{ erg s}^{-1}$). This latter value is consistent with the quiescent state observed in IGR J17544–2619 during a *Chandra* observation [$5.2 \pm 1.3 \times 10^{32} \text{ erg s}^{-1}$, 0.5–10 keV; in’t Zand (2005)], although the two spectra are very different. During the *Chandra* observation the spectrum was very soft, likely thermal (fitted with a power law resulted in a photon index $\Gamma = 5.9 \pm 1.2$), whereas our accumulated spectrum during the very low intensity state is much harder ($\Gamma \sim 1$ –2), very likely implying low rate accretion onto the compact object. The lowest level of X-ray emission ever detected from XTE J1739–302 has been observed with ASCA [$1.1 \times 10^{-12} \text{ erg cm}^{-2} \text{ s}^{-1}$, 2–10 keV; Sakano et al. (2002)], which is much lower than that observed with *Swift*. This comparison, together with the hard spectrum and the small emitting radius (see Table 4) observed with *Swift* implies that we have not reached the quiescent state in this source. Besides IGR J17544–2619, the only other SFXTs where the quiescence (characterized by a soft thermal spectrum and a very low luminosity of $\sim 10^{32} \text{ erg s}^{-1}$) has been caught is IGR J08408–4503 (Leyder et al. 2007).

The low intensity level we observe with *Swift* in IGR J16479–4514 is consistent with it being due to the X-ray eclipses. The possibility of an X-ray eclipse in this transient was originally suggested by Bozzo et al. (2008), based on the variability of the iron line emission observed during an XMM-Newton observation. Then, Jain et al. (2009) found a periodicity at 3.32 days, suggesting it as a possible orbital period. We were able to confirm this periodicity from our independent analysis of the BAT data.

If we assume that this periodicity is of orbital origin, and consider a duration of the X-ray eclipse of 0.6 days (Jain et al. 2009), then the inclination i of the system can be derived from the eclipse semi-angle, θ_e , for an assumed supergiant radius [$R_{\text{OB}} = 23.8 R_{\odot}$ for a O8.5 supergiant, Vacca et al. (1996)] as $R_{\text{OB}} = a \sqrt{(\cos^2 i + \sin^2 i \sin^2 \theta_e)}$. Assuming the system parameters previously adopted for IGR J16479–4514, we obtain a binary separation $a \approx 2 \times 10^{12} \text{ cm}$, implying an orbital inclination of $i \approx 40^\circ$.

This 3.32 days periodicity, if interpreted as the orbital period of the binary system, is puzzling, and is very difficult to rec-

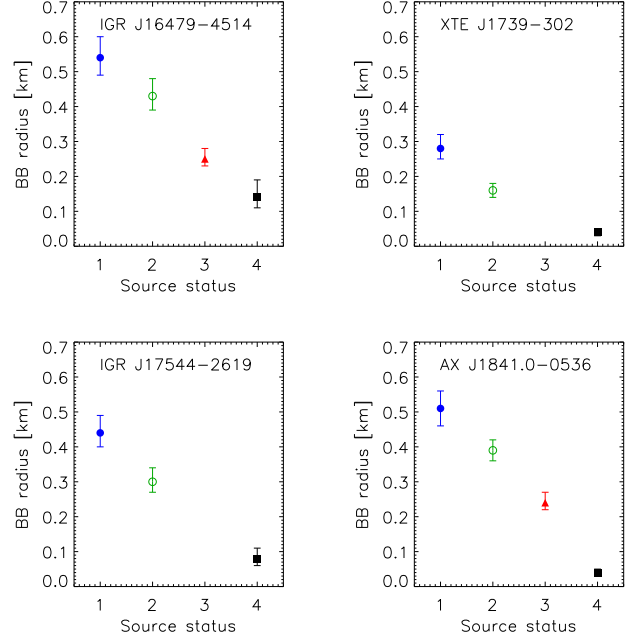


Figure 9. Blackbody radii as a function of source state. The color coding is the same as in Fig. 7 and 8. For the ‘very low’ state, we used the best fits with a constrained N_{H} .

oncle with all the mechanisms proposed to explain the SFXTs phenomenon. The out-of-eclipse average X-ray luminosity of IGR J16479–4514 is $L_{\text{obs}} \approx 10^{34} - 10^{35} \text{ erg s}^{-1}$. It can be compared with the X-ray emission expected from Bondi-Hoyle accretion onto a neutron star. Let us assume a circular orbit (very likely, given the short period), a stellar mass of $M_{\text{OB}} = 30 M_{\odot}$, a radius $R_{\text{OB}} = 23.8 R_{\odot}$ for the supergiant (Vacca et al. 1996), a beta-law velocity for the supergiant wind $v(r) = v_{\infty}(1 - R_{\text{OB}}/r)^{\beta}$ with $\beta = 1$, and a conservative high terminal velocity $v_{\infty} = 2000 \text{ km s}^{-1}$. Under these assumptions the X-ray luminosity produced by the wind accretion for a reasonable choice of the wind mass loss rate ($\dot{M}_{\text{th}} \approx 10^{-6} M_{\odot} \text{ yr}^{-1}$) is $\sim 10^{37} \text{ erg s}^{-1}$, about 2–3 order of magnitude higher than the observed luminosity. On the other hand, the observed low luminosity can be obtained only at a wind mass loss rate of $\dot{M}_{\text{obs}} \approx 10^{-8} - 10^{-9} M_{\odot} \text{ yr}^{-1}$, which is not reasonable for a O8.5 supergiant.

A viable explanation to this inconsistency could be that the 3.32 days periodicity is not orbital, but is only one of the periodicities predicted in our model for the explanation of SFXTs outbursts, that is the time interval between the periodically recurrent flares when the neutron star passes through the preferential plane for the outflowing wind from the supergiant, twice per orbit; thus, the true orbital period can be much longer than this periodicity found [see the different geometries proposed in Sidoli et al. (2007)].

ACKNOWLEDGMENTS

We would like to thank our many collaborators, who helped along the way during this large project, and M. Colpi, who organized a ‘Neutron Star Day’ in Milano in 2006, during which so many new ideas came forth and unexpected collaborations were created... and

who basically got this all started. Then, we would like to thank A. Bazzano, A. Cucchiara, S. Mereghetti, T. Mineo, and P. Ubertini for helpful discussions. We thank the *Swift* team duty scientists and science planners P.J. Brown, M. Chester, S. Hunsberger, J. Racusin, and M.C. Stroh for their dedication and willingness to accommodate our sudden requests in response to outbursts during this monitoring effort. We also thank the remainder of the *Swift* XRT and BAT teams, J.A. Nousek and S. Barthelmy in particular, for their invaluable help and support with the planning and execution of the observing strategy. This work was supported in Italy by contracts ASI I/088/06/0 and I/023/05/0, at PSU by NASA contract NAS5-00136. HAK was supported by the *Swift* project. DNB and JAK acknowledge support from NASA contract NAS5-00136. PR thanks INAF-IASF Milano and LS INAF-IASF Palermo, where some of the work was carried out, for their kind hospitality. We also thank the anonymous referee for comments that helped improve the paper.

REFERENCES

- Bamba A., Yokogawa J., Ueno M., Koyama K., Yamauchi S., 2001, *PASJ*, 53, 1179
- Barthelmy S. D., Barbier L. M., Cummings J. R., et al., 2005, *Space Science Reviews*, 120, 143
- Basko M. M., Sunyaev R. A., & Titarchuk L. G. 1974, *A&A*, 31, 249
- Blay P., Martínez-Núñez S., Negueruela I., et al., 2008, *A&A*, 489, 669
- Bozzo E., Falanga M., Stella L., 2008, *ApJ*, 683, 1031
- Bozzo E., Stella L., Israel G., Falanga M., Campana S., 2008, *MNRAS*, 391, L108
- Burrows D. N., Hill J. E., Nousek J. A., et al., 2005, *Space Science Reviews*, 120, 165
- Cash W., 1979, *ApJ*, 228, 939
- Ducci L., Sidoli L., Paizis A., Mereghetti S., 2008, in proceedings of 7th INTEGRAL Workshop, PoS(Integral08), 086, arXiv:0810.5463
- Gehrels N., Chincarini G., Giommi P., et al., 2004, *ApJ*, 611, 1005
- Hickox R. C., Narayan R., Kallman T. R., 2004, *ApJ*, 614, 881
- Hill J. E., Burrows D. N., Nousek J. A., et al., 2004, in Flanagan K. A., Siegmund O. H. W., eds, *Proceedings of the SPIE, X-Ray and Gamma-Ray Instrumentation for Astronomy XIII*. Volume 5165, p. 217
- in't Zand J. J. M., 2005, *A&A*, 441, L1
- Jain C., Paul B., Dutta A., 2009, *MNRAS*, in press, arXiv:0903.5403
- Krimm H., Barbier L., Barthelmy S. D., et al., 2006, *The Astronomer's Telegram*, 904, 1
- Krimm H. A., Barthelmy S. D., Barbier L., et al., 2007, *Astron. Tel.*, 1265
- Krimm H. A., Barthelmy S. D., Cummings J. R., Markwardt C. B., Skinner G., Tueller J., Swift/BAT Team 2008, in *AAS/High Energy Astrophysics Division Vol. 10 of AAS/High Energy Astrophysics Division, Status of the Swift/BAT Hard X-ray Transient Monitor*. p. #07.01
- Krimm H. A., Romano P., Sidoli L., 2009, *Astron. Tel.*, 1971
- La Parola V., Romano P., Sidoli L., et al., 2009, *Astron. Tel.*, 1929
- Leyder J.-C., Walter R., Lazos M., Masetti N., Produit N., 2007, *A&A*, 465, L35
- Negueruela I., Smith D. M., Harrison T. E., & Torrejón J. M. 2006, *ApJ*, 638, 982
- Negueruela I., Torrejón J. M., Reig P., Ribó M., Smith D. M., 2008, *AIP*, 1010, 252
- Nespoli E., Fabregat J., Mennickent R. E., 2008, *A&A*, 486, 911
- Poole T. S., Breeveld A. A., Page M. J., et al., 2008, *MNRAS*, 383, 627
- Predehl P., Schmitt J. H. M. M., 1995, *A&A*, 293, 889
- Rahoui F., Chaty S., Lagage P.-O., Pantin E., 2008, *A&A*, 484, 801
- Romano P., Cusumano G., Sidoli L., et al., 2008a, *Astron. Tel.*, 1697
- Romano P., Guidorzi C., Sidoli L., et al., 2008b, *Astron. Tel.*, 1659
- Romano P., Sidoli L., Krimm H. A., et al., 2009a, *Astron. Tel.*, 1961
- Romano P., Sidoli L., Mangano V., et al., 2009b, *Astron. Tel.*, 1920
- Romano P., Sidoli L., Mangano V., Mereghetti S., Cusumano G., 2007, *A&A*, 469, L5
- Romano P., Sidoli L., Mangano V., et al., 2008c, *ApJL*, 680, L137 (Paper II)
- Roming P. W. A., Kennedy T. E., Mason K. O., et al., 2005, *Space Science Reviews*, 120, 95
- Sakano M., Koyama K., Murakami H., Maeda Y., Yamauchi S., 2002, *ApJS*, 138, 19
- Sguera V., Barlow E. J., Bird A. J., et al., 2005, *A&A*, 444, 221
- Sguera V., Hill A. B., Bird A. J., Dean A. J., Bazzano A., Ubertini P., Masetti N., Landi R., Malizia A., Clark D. J., Molina M., 2007, *A&A*, 467, 249
- Sguera V., Romero G. E., Bazzano A., Masetti N., Bird A. J., Bassani L., 2009, *ApJ*, in press, arXiv:0903.1763
- Sidoli L., 2009, *Advances in Space Research*, 43, 1464
- Sidoli L., Romano P., Ducci L., et al., 2009a, *MNRAS*, in press, arXiv:0905.2815 (Paper IV)
- Sidoli L., Romano P., Mangano V., et al., 2009b, *ApJ*, 690, 120 (Paper III)
- Sidoli L., Romano P., Mangano V., et al., 2008, *ApJ*, 687, 1230 (Paper I)
- Sidoli L., Romano P., Mereghetti S., Paizis A., Vercellone S., Mangano V., Götz D., 2007, *A&A*, 476, 1307
- Smith D. M., Main D., Marshall F., Swank J., Heindl W. A., Leventhal M., in 't Zand J. J. M., & Heise J., 1998, *ApJL*, 501, L181
- Swank J. H., Smith D. M., Markwardt C. B., 2007, *Astron. Tel.*, 999
- Vacca W. D., Garmany C. D., Shull J. M., 1996, *ApJ*, 460, 914
- Vaughan S., Goad M. R., Beardmore A. P., et al., 2006, *ApJ*, 638, 920
- Walter R., Zurita Heras J., 2007, *A&A*, 476, 335

This paper has been typeset from a $\text{\TeX}/\text{\LaTeX}$ file prepared by the author.

Table 5. Observation log for IGR J16479–4514.

Sequence	Instrument/Mode	Start time (UT) (yyyy-mm-dd hh:mm:ss)	End time (UT) (yyyy-mm-dd hh:mm:ss)	Net Exposure (s)
00030296005	XRT/PC	2007-10-26 08:08:36	2007-10-26 09:42:57	1176
00030296006	XRT/PC	2008-01-19 22:58:28	2008-01-19 23:13:58	927
00030296007	XRT/PC	2008-01-22 20:07:57	2008-01-22 20:25:58	1079
00030296008	XRT/PC	2008-01-26 18:56:04	2008-01-26 19:14:57	1133
00030296009	XRT/PC	2008-01-29 08:03:13	2008-01-29 08:20:56	1062
00030296010	XRT/PC	2008-02-05 00:48:59	2008-02-05 16:58:56	3056
00030296011	XRT/PC	2008-02-09 18:53:39	2008-02-09 23:50:58	2749
00030296012	XRT/PC	2008-02-10 01:16:40	2008-02-10 04:36:58	873
00030296013	XRT/PC	2008-02-15 08:12:38	2008-02-15 10:01:25	1254
00030296014	XRT/PC	2008-02-18 06:49:05	2008-02-18 10:12:57	804
00030296015	XRT/PC	2008-02-20 00:33:38	2008-02-20 00:46:58	798
00030296016	XRT/PC	2008-02-23 21:44:31	2008-02-23 23:35:57	1667
00030296017	XRT/PC	2008-02-26 23:38:06	2008-02-26 23:52:56	890
00030296018	XRT/PC	2008-03-01 23:38:51	2008-03-01 23:59:59	1266
00030296019	XRT/PC	2008-03-03 01:50:45	2008-03-03 05:07:56	1083
00030296020	XRT/PC	2008-03-06 00:26:49	2008-03-06 02:12:58	1098
00030296021	XRT/PC	2008-03-10 09:05:42	2008-03-10 12:15:56	1261
00030296022	XRT/PC	2008-03-11 20:00:41	2008-03-11 23:22:56	2985
00030296023	XRT/PC	2008-03-12 18:46:44	2008-03-12 23:51:49	2796
00030296024	XRT/PC	2008-03-13 04:14:40	2008-03-13 04:34:56	1213
00030296025	XRT/PC	2008-03-15 04:37:49	2008-03-15 04:55:57	1086
00030296026	XRT/PC	2008-03-16 07:56:54	2008-03-16 08:15:30	1116
00030296027	XRT/PC	2008-03-17 06:34:08	2008-03-17 08:21:48	1215
00030296028	XRT/PC	2008-03-18 06:31:54	2008-03-18 16:21:56	2333
00030296029	XRT/WT	2008-03-19 19:38:51	2008-03-19 22:46:00	67
00030296029	XRT/PC	2008-03-19 19:38:56	2008-03-19 19:47:57	542
00306829000	XRT/WT	2008-03-19 22:46:47	2008-03-19 23:55:26	884
00306829000	XRT/PC	2008-03-19 23:55:27	2008-03-20 00:00:53	304
00030296030	XRT/PC	2008-03-21 02:05:29	2008-03-21 03:48:58	835
00030296031	XRT/PC	2008-03-21 21:22:28	2008-03-21 23:05:57	835
00030296032	XRT/PC	2008-03-23 05:25:03	2008-03-23 05:35:30	625
00030296033	XRT/PC	2008-03-24 05:36:51	2008-03-24 06:50:56	1040
00030296034	XRT/PC	2008-04-10 15:17:37	2008-04-10 20:10:57	905
00030296035	XRT/PC	2008-05-02 22:12:26	2008-05-02 22:25:56	809
00030296036	XRT/PC	2008-05-06 20:40:14	2008-05-06 20:43:39	205
00030296037	XRT/PC	2008-05-10 09:53:10	2008-05-10 10:10:56	1066
00030296038	XRT/PC	2008-05-14 08:33:12	2008-05-14 08:52:58	1186
00030296039	XRT/PC	2008-05-22 20:54:24	2008-05-22 22:45:56	2379
00030296040	XRT/PC	2008-05-26 21:05:40	2008-05-26 21:28:57	1396
00030296041	XRT/PC	2008-05-30 08:40:01	2008-05-31 18:10:58	995
00030296042	XRT/PC	2008-06-03 20:15:44	2008-06-03 20:34:57	1153
00030296043	XRT/PC	2008-06-07 16:05:45	2008-06-07 16:09:56	250
00030296044	XRT/PC	2008-06-11 08:22:02	2008-06-11 09:57:56	985
00030296046	XRT/PC	2008-06-19 17:03:51	2008-06-19 18:51:58	1510
00030296047	XRT/PC	2008-06-23 09:12:34	2008-06-23 09:25:56	802
00030296048	XRT/PC	2008-06-28 00:35:19	2008-06-28 04:59:57	970
00030296049	XRT/PC	2008-07-01 05:12:34	2008-07-01 05:28:57	982
00030296050	XRT/PC	2008-07-05 13:53:11	2008-07-05 14:10:57	1066
00030296052	XRT/PC	2008-07-13 09:51:01	2008-07-13 11:34:56	948
00030296053	XRT/PC	2008-07-17 13:26:34	2008-07-17 13:30:44	250
00030296055	XRT/PC	2008-07-21 02:13:37	2008-07-21 02:29:57	980
00030296056	XRT/PC	2008-07-25 02:53:34	2008-07-25 03:10:57	1043
00030296057	XRT/PC	2008-07-29 09:41:29	2008-07-29 09:58:57	1048
00030296058	XRT/PC	2008-08-02 13:00:42	2008-08-02 14:46:58	933
00030296059	XRT/PC	2008-08-06 02:09:08	2008-08-06 02:25:56	1007
00030296060	XRT/PC	2008-08-10 00:57:00	2008-08-10 01:11:57	896

Table 5. Observation log for IGR J16479–4514. Continued

Sequence	Instrument/Mode	Start time (UT) (yyyy-mm-dd hh:mm:ss)	End time (UT) (yyyy-mm-dd hh:mm:ss)	Net Exposure (s)
00030296061	XRT/PC	2008-08-14 19:10:16	2008-08-14 19:25:56	939
00030296062	XRT/PC	2008-08-18 11:27:53	2008-08-18 11:43:56	963
00030296063	XRT/PC	2008-08-22 07:01:50	2008-08-22 23:07:57	755
00030296065	XRT/PC	2008-08-30 01:29:10	2008-08-30 03:15:56	1236
00030296066	XRT/PC	2008-09-11 23:18:06	2008-09-11 23:32:56	890
00030296067	XRT/PC	2008-09-15 07:46:25	2008-09-15 08:02:56	990
00030296070	XRT/PC	2008-09-27 05:41:07	2008-09-27 05:58:55	1068
00030296071	XRT/PC	2008-10-01 15:49:11	2008-10-01 16:07:57	1126
00030296073	XRT/PC	2008-10-12 23:14:15	2008-10-12 23:28:55	880
00030296074	XRT/PC	2008-10-17 01:27:07	2008-10-17 03:05:57	471
00030296075	XRT/PC	2008-10-21 04:46:15	2008-10-21 05:00:57	883
00030296076	XRT/PC	2008-10-25 22:48:38	2008-10-25 23:02:05	805
00341452000	XRT/WT	2009-01-29 06:46:53	2009-01-29 08:16:49	46
00341452000	XRT/PC	2009-01-29 06:47:35	2009-01-29 08:39:04	2628
00030296077	XRT/PC	2009-01-29 15:59:44	2009-01-29 22:36:24	5911
00030296078	XRT/PC	2009-01-30 05:05:45	2009-01-30 07:01:56	2477
00030296079	XRT/PC	2009-01-31 00:23:45	2009-01-31 02:17:58	1363
00030296080	XRT/PC	2009-02-01 19:50:46	2009-02-01 21:30:57	2022
00030296081	XRT/PC	2009-02-02 08:46:12	2009-02-02 11:40:57	1886
00030296082	XRT/PC	2009-02-03 18:25:48	2009-02-03 21:49:58	1215
00030296083	XRT/PC	2009-02-04 00:51:50	2009-02-04 04:09:56	1403
00030296084	XRT/PC	2009-02-05 02:24:25	2009-02-05 02:50:30	1507
00030296085	XRT/PC	2009-02-06 01:13:12	2009-02-06 04:28:57	486
00030296087	XRT/PC	2009-02-08 18:54:08	2009-02-08 22:15:57	1605
00030296088	XRT/PC	2009-02-10 03:10:18	2009-02-10 08:06:57	1542
00030296089	XRT/PC	2009-02-11 15:47:39	2009-02-11 22:38:57	2242
00030296090	XRT/PC	2009-02-12 22:30:18	2009-02-13 00:20:56	1683
00030296091	XRT/PC	2009-02-13 05:04:18	2009-02-13 06:45:54	1301
00030296092	XRT/PC	2009-02-14 06:34:01	2009-02-14 08:18:56	1270
00030296093	XRT/PC	2009-02-15 03:19:41	2009-02-15 03:39:57	1202
00030296094	XRT/PC	2009-02-16 08:26:29	2009-02-16 10:14:42	1126
00030296095	XRT/PC	2009-02-17 00:22:55	2009-02-17 00:38:50	952

Table 6. Observation log for IGR J17391–3021.

Sequence	Instrument/Mode	Start time (UT) (yyyy-mm-dd hh:mm:ss)	End time (UT) (yyyy-mm-dd hh:mm:ss)	Net Exposure (s)
00030987001	XRT/PC	2007-10-27 09:46:16	2007-10-27 10:05:57	1181
00030987002	XRT/PC	2007-10-30 10:12:32	2007-10-30 10:25:57	805
00030987003	XRT/PC	2007-11-01 08:47:14	2007-11-01 09:06:58	1181
00030987004	XRT/PC	2008-02-04 21:24:07	2008-02-04 22:57:58	940
00030987005	XRT/PC	2008-02-06 00:48:04	2008-02-06 23:29:58	5606
00030987006	XRT/PC	2008-02-08 01:10:03	2008-02-08 02:48:58	161
00030987007	XRT/PC	2008-02-11 17:26:01	2008-02-11 19:16:56	1295
00030987008	XRT/PC	2008-02-13 09:48:13	2008-02-13 11:30:54	180
00030987009	XRT/PC	2008-02-15 06:32:34	2008-02-15 06:40:58	504
00030987010	XRT/PC	2008-02-18 03:45:06	2008-02-18 05:26:56	498
00030987011	XRT/PC	2008-02-21 00:40:01	2008-02-21 00:57:57	1076
00030987012	XRT/PC	2008-02-22 00:52:08	2008-02-22 01:06:55	888
00030987013	XRT/PC	2008-02-25 17:19:52	2008-02-25 19:03:57	597
00030987014	XRT/PC	2008-02-27 01:26:01	2008-02-27 03:05:57	937
00030987015	XRT/PC	2008-02-28 01:23:19	2008-02-28 01:40:57	1056
00030987016	XRT/PC	2008-03-03 21:06:00	2008-03-03 21:22:58	1016
00030987017	XRT/PC	2008-03-05 21:21:59	2008-03-05 22:55:57	1244
00030987018	XRT/PC	2008-03-08 04:03:06	2008-03-08 12:12:57	2821
00030987019	XRT/PC	2008-03-10 18:43:52	2008-03-10 20:25:56	647
00030987020	XRT/PC	2008-03-11 12:16:41	2008-03-11 18:54:58	2908
00030987021	XRT/PC	2008-03-14 09:21:55	2008-03-14 09:40:50	1108
00030987022	XRT/PC	2008-03-16 17:34:59	2008-03-16 17:51:57	1018
00030987023	XRT/PC	2008-03-19 00:28:15	2008-03-19 03:45:50	672
00030987024	XRT/PC	2008-03-21 05:18:20	2008-03-22 00:41:56	1043
00030987025	XRT/PC	2008-03-23 23:14:57	2008-03-24 20:17:57	1257
00030987026	XRT/PC	2008-03-30 23:41:20	2008-03-30 23:57:58	996
00030987027	XRT/PC	2008-04-02 03:08:26	2008-04-02 03:24:56	990
00030987028	XRT/PC	2008-04-07 16:27:21	2008-04-07 16:43:56	995
00308797000	BAT/evt	2008-04-08 21:24:16	2008-04-08 23:09:11	1735
00308797000	XRT/WT	2008-04-08 21:34:47	2008-04-08 23:09:19	128
00308797000	XRT/PC	2008-04-08 21:36:54	2008-04-08 23:19:19	938
00030987029	XRT/PC	2008-04-19 06:26:23	2008-04-19 08:09:56	908
00030987030	XRT/PC	2008-04-21 19:28:21	2008-04-21 21:15:57	1146
00030987031	XRT/PC	2008-04-23 02:03:03	2008-04-23 02:14:58	689
00030987032	XRT/PC	2008-04-28 10:26:57	2008-04-28 10:42:57	960
00030987033	XRT/PC	2008-04-30 13:58:59	2008-04-30 14:14:57	958
00030987034	XRT/PC	2008-05-05 16:08:11	2008-05-05 16:22:56	885
00030987035	XRT/PC	2008-05-07 16:19:15	2008-05-07 16:34:58	941
00030987036	XRT/PC	2008-05-09 16:27:21	2008-05-09 16:43:56	995
00030987037	XRT/PC	2008-05-12 08:21:50	2008-05-12 08:40:56	1146
00030987038	XRT/PC	2008-05-14 00:32:06	2008-05-14 00:51:57	1191
00030987040	XRT/PC	2008-05-24 20:51:34	2008-05-24 21:12:58	1282
00030987041	XRT/PC	2008-05-26 22:49:18	2008-05-26 23:08:56	1178
00030987042	XRT/PC	2008-05-28 11:27:22	2008-05-28 11:45:58	1116
00030987043	XRT/PC	2008-05-30 10:18:29	2008-05-30 10:30:56	746
00030987044	XRT/PC	2008-06-02 16:57:25	2008-06-02 20:37:56	1269
00030987045	XRT/PC	2008-06-04 06:00:05	2008-06-04 06:18:56	1131
00030987047	XRT/PC	2008-06-09 17:54:23	2008-06-09 18:03:57	572
00030987048	XRT/PC	2008-06-11 06:45:09	2008-06-11 07:00:56	948
00030987049	XRT/PC	2008-06-12 18:12:07	2008-06-12 23:07:57	943
00030987050	XRT/PC	2008-06-13 10:04:48	2008-06-13 10:20:56	968
00030987051	XRT/PC	2008-06-16 00:37:58	2008-06-16 00:57:56	1198
00030987052	XRT/WT	2008-06-21 07:38:11	2008-06-21 14:00:10	53
00030987052	XRT/PC	2008-06-21 07:38:53	2008-06-21 14:10:56	2517
00030987053	XRT/PC	2008-06-23 09:26:58	2008-06-23 09:35:58	538
00030987054	XRT/PC	2008-06-25 01:38:49	2008-06-25 08:02:58	1863
00030987055	XRT/PC	2008-07-04 15:29:32	2008-07-04 15:46:55	1043
00030987056	XRT/PC	2008-07-07 10:49:25	2008-07-07 11:06:48	1043
00030987057	XRT/PC	2008-07-09 12:51:21	2008-07-09 13:02:55	695
00030987058	XRT/PC	2008-07-11 12:41:02	2008-07-11 12:56:57	954
00030987059	XRT/PC	2008-07-19 05:23:41	2008-07-19 07:07:57	992
00030987060	XRT/PC	2008-07-21 20:28:02	2008-07-21 20:34:56	414

Table 6. Observation log for IGR J17391–3021. Continued.

Sequence	Instrument/Mode	Start time (UT) (yyyy-mm-dd hh:mm:ss)	End time (UT) (yyyy-mm-dd hh:mm:ss)	Net Exposure (s)
00030987061	XRT/PC	2008-07-23 17:18:27	2008-07-23 17:28:09	579
00030987062	XRT/PC	2008-07-25 04:29:36	2008-07-25 06:14:56	948
00030987063	XRT/PC	2008-07-28 07:58:32	2008-07-28 09:42:56	953
00030987064	XRT/PC	2008-07-30 19:27:28	2008-07-30 21:12:55	1076
00030987067	XRT/PC	2008-08-06 23:17:02	2008-08-06 23:38:56	1314
00030987068	XRT/PC	2008-08-08 12:09:29	2008-08-08 12:32:56	1407
00030987069	XRT/PC	2008-08-10 02:45:41	2008-08-10 03:03:57	1094
00319963000	XRT/WT	2008-08-13 23:55:55	2008-08-14 00:29:09	1688
00319963000	XRT/PC	2008-08-14 00:03:19	2008-08-14 00:04:34	75
00030987070	XRT/WT	2008-08-14 01:23:10	2008-08-14 13:03:50	1207
00030987070	XRT/PC	2008-08-14 04:36:11	2008-08-14 13:17:16	10714
00030987071	XRT/PC	2008-08-15 00:00:34	2008-08-15 00:16:57	983
00030987072	XRT/PC	2008-08-16 03:21:09	2008-08-16 05:08:57	1379
00030987073	BAT/PC	2008-08-17 01:44:09	2008-08-17 02:01:57	1068
00030987074	XRT/PC	2008-08-18 13:04:08	2008-08-18 13:21:56	1068
00030987075	XRT/PC	2008-08-19 13:09:42	2008-08-19 13:27:58	1095
00030987076	XRT/PC	2008-08-20 05:14:06	2008-08-20 05:31:56	1071
00030987077	XRT/PC	2008-08-21 00:30:30	2008-08-21 15:08:55	1173
00030987078	XRT/PC	2008-08-22 00:36:19	2008-08-22 02:21:55	1093
00030987079	XRT/PC	2008-08-23 03:55:11	2008-08-23 05:41:56	1229
00030987080	XRT/PC	2008-08-24 21:44:19	2008-08-24 23:31:57	1332
00030987081	XRT/PC	2008-08-25 21:50:21	2008-08-25 23:35:56	1274
00030987082	XRT/PC	2008-08-27 13:55:09	2008-08-27 14:15:58	1249
00030987083	XRT/PC	2008-08-29 09:16:27	2008-08-29 11:10:58	2221
00030987084	XRT/PC	2008-08-31 14:18:01	2008-08-31 14:36:57	1136
00030987085	BAT/PC	2008-09-04 06:45:52	2008-09-04 07:06:56	1263
00030987086	XRT/PC	2008-09-13 10:44:42	2008-09-13 23:48:56	1047
00030987087	XRT/PC	2008-09-16 22:18:49	2008-09-16 22:23:35	286
00030987088	XRT/PC	2008-09-25 05:31:25	2008-09-25 05:47:56	990
00030987089	XRT/PC	2008-09-29 09:05:25	2008-09-29 09:21:56	990
00030987091	XRT/PC	2008-10-07 19:33:16	2008-10-07 19:50:57	1061
00030987092	XRT/PC	2008-10-11 23:08:23	2008-10-11 23:21:55	812
00030987093	XRT/PC	2008-10-15 18:42:46	2008-10-15 20:22:56	815
00030987094	XRT/PC	2008-10-19 15:50:55	2008-10-19 19:11:56	1081
00030987095	XRT/PC	2008-10-23 00:09:33	2008-10-23 00:22:58	803
00030987096	XRT/PC	2008-10-27 19:50:03	2008-10-27 21:33:56	875
00030987097	XRT/PC	2008-10-31 00:57:26	2008-10-31 01:13:56	990

Table 7. Observation log for IGR J17544–2619.

Sequence	Instrument/Mode	Start time (UT) (yyyy-mm-dd hh:mm:ss)	End time (UT) (yyyy-mm-dd hh:mm:ss)	Net Exposure (s)
00035056002	XRT/PC	2007-10-28 00:20:09	2007-10-29 07:07:56	2783
00035056003	XRT/PC	2007-10-31 10:19:05	2007-10-31 13:43:35	248
00035056004	XRT/PC	2007-11-04 00:58:32	2007-11-04 01:16:58	1104
00035056005	XRT/PC	2008-02-07 20:17:58	2008-02-07 23:43:57	1331
00035056006	XRT/PC	2008-02-10 19:14:07	2008-02-10 20:52:56	278
00035056007	XRT/PC	2008-02-14 08:17:17	2008-02-14 10:00:56	915
00035056008	XRT/PC	2008-02-17 00:16:44	2008-02-17 02:04:56	1346
00035056009	XRT/PC	2008-02-21 10:24:08	2008-02-21 10:40:36	960
00035056010	XRT/PC	2008-02-24 23:41:09	2008-02-25 01:24:57	998
00035056011	XRT/PC	2008-02-28 02:41:54	2008-02-28 02:58:57	1004
00035056012	XRT/PC	2008-03-03 22:43:07	2008-03-03 23:00:57	1071
00035056013	XRT/PC	2008-03-06 03:52:22	2008-03-06 07:13:58	1180
00035056014	XRT/PC	2008-03-10 13:54:43	2008-03-10 17:13:58	627
00035056015	XRT/PC	2008-03-13 22:06:37	2008-03-13 23:42:56	1296
00035056016	XRT/PC	2008-03-16 04:43:43	2008-03-16 06:33:56	1701
00035056017	XRT/PC	2008-03-20 12:57:18	2008-03-20 13:07:58	639
00035056018	XRT/PC	2008-03-23 18:20:14	2008-03-23 18:36:56	1002
00035056019	XRT/PC	2008-03-27 00:45:04	2008-03-27 01:02:57	1073
00035056020	XRT/PC	2008-03-31 03:07:59	2008-03-31 04:52:57	898
00308224000	BAT/evt	2008-03-31 20:46:48	2008-03-31 21:06:50	1202
00308224000	XRT/WT	2008-03-31 20:53:35	2008-03-31 20:58:57	306
00035056021	XRT/PC	2008-03-31 21:52:49	2008-03-31 22:17:41	1492
00035056022	XRT/PC	2008-04-02 22:29:22	2008-04-02 22:42:57	815
00035056024	XRT/PC	2008-04-03 05:05:00	2008-04-03 06:47:56	1098
00035056025	XRT/PC	2008-04-06 05:12:15	2008-04-06 05:28:58	1000
00035056026	XRT/PC	2008-04-10 21:46:21	2008-04-10 23:30:56	1027
00035056027	XRT/PC	2008-04-13 01:12:20	2008-04-13 02:54:28	765
00035056028	XRT/PC	2008-04-17 20:45:21	2008-04-17 22:34:57	1030
00035056029	XRT/PC	2008-04-20 16:21:01	2008-04-20 19:36:56	888
00035056030	XRT/PC	2008-04-28 13:44:33	2008-04-28 14:00:56	983
00035056031	XRT/PC	2008-05-01 19:04:49	2008-05-01 20:48:56	925
00035056032	XRT/PC	2008-05-04 19:20:41	2008-05-04 19:30:58	615
00035056033	XRT/PC	2008-05-11 16:18:15	2008-05-11 16:35:58	1061
00035056035	XRT/PC	2008-05-29 11:56:34	2008-05-29 13:40:56	1122
00035056036	XRT/PC	2008-06-01 01:05:55	2008-06-01 02:46:56	1091
00035056037	XRT/PC	2008-06-08 21:01:29	2008-06-08 21:12:56	687
00035056038	XRT/PC	2008-06-12 19:49:25	2008-06-12 21:35:57	1269
00035056040	XRT/PC	2008-06-22 16:04:17	2008-06-22 17:49:56	1098
00035056041	XRT/PC	2008-06-26 10:03:44	2008-06-26 11:48:57	1274
00035056042	XRT/PC	2008-06-29 00:48:45	2008-06-29 02:27:57	607
00035056043	XRT/PC	2008-07-03 13:54:30	2008-07-03 15:37:57	1071
00035056044	XRT/PC	2008-07-06 18:50:24	2008-07-06 19:10:57	1232
00035056045	XRT/PC	2008-07-10 12:48:28	2008-07-10 12:52:21	232
00035056046	XRT/PC	2008-07-13 13:03:40	2008-07-13 14:47:56	945
00035056047	XRT/PC	2008-07-18 00:57:56	2008-07-18 02:10:56	900
00035056048	XRT/PC	2008-07-20 10:33:42	2008-07-20 10:52:56	1153
00035056049	XRT/PC	2008-07-24 12:34:50	2008-07-24 12:37:33	163
00035056051	XRT/PC	2008-07-31 01:46:30	2008-07-31 02:02:56	985
00035056052	XRT/PC	2008-08-03 10:14:34	2008-08-03 10:34:57	1222
00035056053	XRT/PC	2008-08-07 15:10:57	2008-08-07 15:14:56	238
00035056054	XRT/PC	2008-08-10 04:22:25	2008-08-10 05:55:58	1320
00035056055	XRT/PC	2008-08-14 20:46:21	2008-08-14 21:02:57	994
00035056056	XRT/PC	2008-08-17 03:20:43	2008-08-17 03:38:56	1093
00035056057	XRT/PC	2008-08-21 16:34:57	2008-08-21 18:15:55	1015
00035056058	XRT/PC	2008-08-24 18:37:32	2008-08-24 18:53:55	983
00035056059	XRT/PC	2008-08-29 23:52:42	2008-08-30 05:05:58	993
00035056060	XRT/PC	2008-08-31 15:57:58	2008-08-31 22:25:57	1191

Table 7. Observation log for IGR J17544–2619. Continued.

Sequence	Instrument/Mode	Start time (UT) (yyyy-mm-dd hh:mm:ss)	End time (UT) (yyyy-mm-dd hh:mm:ss)	Net Exposure (s)
00035056061	XRT/PC	2008-09-04 00:12:45	2008-09-04 00:26:55	632
00035056061	XRT/WT	2008-09-04 00:12:40	2008-09-04 00:25:03	217
00035056062	XRT/PC	2008-09-05 05:22:27	2008-09-05 11:44:56	2521
00035056065	XRT/PC	2008-09-11 09:05:46	2008-09-11 10:44:55	923
00035056066	XRT/PC	2008-09-12 12:28:46	2008-09-12 12:44:56	970
00035056067	XRT/PC	2008-09-13 12:23:36	2008-09-13 14:13:56	900
00035056068	XRT/PC	2008-09-14 12:31:39	2008-09-14 14:18:55	905
00035056069	XRT/PC	2008-09-15 10:54:20	2008-09-15 12:45:55	958
00035056070	XRT/PC	2008-09-16 22:12:44	2008-09-16 23:59:57	930
00035056071	XRT/PC	2008-09-19 00:03:19	2008-09-19 00:04:34	75
00035056072	XRT/PC	2008-09-22 02:02:35	2008-09-22 02:24:56	1341
00035056073	XRT/PC	2008-09-26 13:39:41	2008-09-26 13:48:27	527
00035056074	XRT/PC	2008-09-30 07:33:35	2008-09-30 07:50:55	1041
00035056075	XRT/PC	2008-10-04 01:41:09	2008-10-04 01:55:56	888
00035056076	XRT/PC	2008-10-08 11:37:00	2008-10-08 14:55:56	1248
00035056077	XRT/PC	2008-10-12 20:01:34	2008-10-12 21:43:57	644
00035056078	XRT/PC	2008-10-16 06:21:58	2008-10-16 06:35:58	839
00035056079	XRT/PC	2008-10-20 09:30:55	2008-10-20 11:20:58	1683
00035056080	XRT/PC	2008-10-25 05:11:59	2008-10-25 06:58:56	1249
00035056081	XRT/PC	2008-10-28 07:08:43	2008-10-28 10:23:57	506
00035056082	XRT/PC	2008-10-31 01:14:50	2008-10-31 01:30:58	967

Table 8. Observation log for IGR J18410–0535.

Sequence	Instrument/Mode	Start time (UT) (yyyy-mm-dd hh:mm:ss)	End time (UT) (yyyy-mm-dd hh:mm:ss)	Net Exposure (s)
00030988001	XRT/PC	2007-10-26 00:08:53	2007-10-26 06:45:56	1384
00030988002	XRT/PC	2007-10-28 22:53:11	2007-10-29 23:12:56	3199
00030988003	XRT/PC	2007-11-03 10:37:52	2007-11-03 12:24:56	1122
00030988004	XRT/PC	2007-11-05 09:08:39	2007-11-05 09:28:58	1218
00030988005	XRT/PC	2007-11-09 16:11:30	2007-11-09 16:32:56	1286
00030988006	XRT/PC	2007-11-12 14:51:25	2007-11-12 14:51:55	30
00030988007	XRT/PC	2007-11-16 08:40:04	2007-11-16 10:36:58	2332
00030988008	XRT/PC	2007-11-18 23:22:32	2007-11-18 23:41:58	1165
00030988009	XRT/PC	2008-02-14 14:44:51	2008-02-14 16:28:58	947
00030988009	XRT/WT	2008-02-14 14:42:45	2008-02-14 16:20:15	127
00030988010	XRT/PC	2008-02-18 00:26:32	2008-02-18 02:13:57	626
00030988011	XRT/PC	2008-02-21 08:46:13	2008-02-21 09:02:58	1005
00030988012	XRT/PC	2008-02-25 20:32:34	2008-02-25 20:47:57	834
00030988013	XRT/PC	2008-02-28 03:00:08	2008-02-28 03:16:56	1008
00030988014	XRT/PC	2008-03-03 17:54:04	2008-03-03 17:56:45	160
00030988015	XRT/PC	2008-03-06 08:41:40	2008-03-06 12:00:57	1374
00030988016	XRT/PC	2008-03-10 10:49:43	2008-03-10 23:20:57	2031
00030988017	XRT/PC	2008-03-13 05:59:01	2008-03-13 06:20:58	1316
00030988018	XRT/PC	2008-03-17 00:12:23	2008-03-17 01:54:57	1143
00030988019	XRT/PC	2008-03-20 17:56:07	2008-03-20 18:16:58	1249
00030988020	XRT/PC	2008-03-24 02:22:04	2008-03-24 04:07:56	1173
00030988021	XRT/PC	2008-03-27 01:04:11	2008-03-27 01:19:56	944
00030988022	XRT/PC	2008-03-31 01:25:11	2008-03-31 01:41:57	1005
00030988023	XRT/PC	2008-04-03 08:17:07	2008-04-03 10:02:49	973
00030988024	XRT/PC	2008-04-07 05:18:10	2008-04-07 05:34:56	1005
00030988026	XRT/PC	2008-04-17 12:52:27	2008-04-17 14:35:56	1078
00030988027	XRT/PC	2008-04-21 08:14:08	2008-04-21 08:31:56	1068
00030988029	XRT/PC	2008-04-28 08:51:35	2008-04-28 09:07:56	980
00030988030	XRT/PC	2008-05-01 15:53:55	2008-05-01 17:37:56	845
00030988031	XRT/PC	2008-05-05 12:54:44	2008-05-05 14:44:58	925
00030988032	XRT/PC	2008-05-08 03:10:56	2008-05-08 05:23:57	888
00030988033	XRT/PC	2008-05-12 01:57:30	2008-05-12 02:14:58	1048
00030988034	XRT/PC	2008-05-15 12:14:47	2008-05-15 13:54:56	1081
00030988035	XRT/PC	2008-05-22 03:22:44	2008-05-22 03:29:58	434
00030988036	XRT/PC	2008-05-26 19:23:27	2008-05-26 19:42:58	1171
00030988037	XRT/PC	2008-05-29 00:43:05	2008-05-29 19:59:58	1402
00030988038	XRT/PC	2008-06-02 12:01:25	2008-06-02 12:17:58	991
00030988039	XRT/PC	2008-06-01 07:37:34	2008-06-02 20:21:56	1263
00030988041	XRT/PC	2008-06-11 13:03:36	2008-06-11 13:18:56	920
00030988042	XRT/PC	2008-06-18 07:26:24	2008-06-18 07:46:57	1234
00030988043	XRT/PC	2008-06-21 07:28:07	2008-06-21 13:57:58	2188
00030988044	XRT/PC	2008-06-23 04:28:01	2008-06-23 07:46:55	1301
00030988045	XRT/PC	2008-06-25 01:57:19	2008-06-25 08:18:55	1123
00030988046	XRT/PC	2008-06-28 13:13:57	2008-06-28 13:30:57	1020
00030988047	XRT/PC	2008-06-30 21:50:01	2008-06-30 21:50:56	54
00030988048	XRT/PC	2008-07-04 13:32:01	2008-07-04 13:49:57	1075
00030988049	XRT/PC	2008-07-07 12:13:17	2008-07-07 12:30:55	1058
00030988050	XRT/PC	2008-07-09 19:03:33	2008-07-09 19:06:56	203
00030988051	XRT/PC	2008-07-11 00:16:45	2008-07-11 01:59:56	604
00030988052	XRT/PC	2008-07-14 13:09:38	2008-07-14 16:27:57	963
00030988053	XRT/PC	2008-07-16 00:42:49	2008-07-16 02:31:57	1214
00030988054	XRT/PC	2008-07-18 18:17:53	2008-07-18 18:36:56	1143
00030988055	XRT/PC	2008-07-21 22:04:43	2008-07-21 22:16:58	734
00030988056	XRT/PC	2008-07-23 19:15:35	2008-07-23 19:15:58	21
00030988057	XRT/PC	2008-07-25 00:02:37	2008-07-25 01:42:58	1088
00030988058	XRT/PC	2008-07-28 06:32:48	2008-07-28 06:35:56	187
00030988059	XRT/PC	2008-07-30 11:38:47	2008-07-30 11:52:57	850
00030988059	XRT/WT	2008-07-30 11:38:14	2008-07-30 11:38:45	31
00030988060	XRT/PC	2008-08-01 18:05:50	2008-08-01 18:21:58	968

Table 8. Observation log for IGR J18410–0535. Continued

Sequence	Instrument/Mode	Start time (UT) (yyyy-mm-dd hh:mm:ss)	End time (UT) (yyyy-mm-dd hh:mm:ss)	Net Exposure (s)
00030988061	XRT/PC	2008-08-03 15:26:25	2008-08-04 20:08:57	1051
00030988062	XRT/PC	2008-08-06 18:32:32	2008-08-06 18:49:55	1043
00030988064	XRT/PC	2008-08-11 12:25:28	2008-08-11 12:40:10	883
00030988065	XRT/PC	2008-08-16 08:05:17	2008-08-16 08:21:58	1000
00030988066	XRT/PC	2008-08-18 10:10:52	2008-08-18 10:26:57	965
00030988067	XRT/PC	2008-08-20 06:51:23	2008-08-20 07:07:56	993
00030988068	XRT/PC	2008-08-22 03:50:07	2008-08-22 05:32:56	930
00030988069	XRT/PC	2008-08-25 07:32:25	2008-08-25 08:00:57	1712
00030988070	XRT/PC	2008-08-27 12:19:48	2008-08-27 12:38:56	1148
00030988071	XRT/PC	2008-08-30 06:24:02	2008-08-30 06:39:57	955
00030988072	XRT/PC	2008-08-31 23:58:41	2008-09-01 04:57:57	2579
00030988073	XRT/PC	2008-09-03 00:10:17	2008-09-03 03:47:57	1224
00030988074	XRT/PC	2008-09-05 13:18:16	2008-09-05 13:30:56	760
00030988075	XRT/PC	2008-09-08 10:22:05	2008-09-08 12:09:56	1379
00030988076	XRT/PC	2008-09-12 14:01:24	2008-09-12 14:17:57	993
00030988077	XRT/PC	2008-09-15 19:18:47	2008-09-15 19:33:57	910
00030988078	XRT/PC	2008-09-17 08:03:00	2008-09-17 11:28:58	988
00030988079	XRT/PC	2008-09-24 18:33:17	2008-09-24 20:19:57	1399
00030988080	XRT/PC	2008-09-28 17:25:46	2008-09-28 19:09:56	1106
00030988081	XRT/PC	2008-10-02 17:31:43	2008-10-02 17:48:56	1033
00030988082	XRT/PC	2008-10-06 00:11:19	2008-10-06 00:28:58	984
00030988083	XRT/PC	2008-10-10 13:41:49	2008-10-10 13:57:56	968
00030988085	XRT/PC	2008-10-17 04:58:39	2008-10-17 06:30:56	1632
00030988086	XRT/PC	2008-10-22 20:57:48	2008-10-22 22:46:57	1582
00030988087	XRT/PC	2008-10-26 00:30:59	2008-10-26 08:40:12	940
00030988088	XRT/PC	2008-10-30 21:44:03	2008-10-30 22:02:56	1133
00030988089	XRT/PC	2008-11-02 01:30:42	2008-11-02 01:49:56	1153
00030988090	XRT/PC	2008-11-08 01:42:41	2008-11-08 03:29:57	1324
00030988091	XRT/PC	2008-11-12 05:29:21	2008-11-12 08:52:56	2091
00030988092	XRT/PC	2008-11-15 08:50:09	2008-11-15 09:11:58	1309